A differential effect for tau isoforms and mutants in decreasing the stability of Arc

Dina W. Yakout[1], Ankit Shroff[2], Zachary D. Allen[1], Taras Y. Nazarko[2], Angela M. Mabb[1,3*]

[1]Neuroscience Institute, Georgia State University, Atlanta, Georgia, United States.
[2]Department of Biology, Georgia State University, Atlanta, Georgia, United States.
[3]Center for Behavioral Neuroscience, Atlanta, Georgia, United States.

*Correspondence:
Dr. Angela M. Mabb
Georgia State University
100 Piedmont Ave. SE
Atlanta, GA 30303
USA
Tel: 404.413.6306
FAX: 404.413.5446
e-mail: amabb@gsu.edu

Keywords:

Arc, tau, AMPA receptors, proteasome, ubiquitination, Alzheimer's disease

Abstract

Tauopathies are neurodegenerative disorders characterized by the deposition of aggregates of the microtubule associated protein tau, a main component of neurofibrillary tangles. Alzheimer's disease (AD) is the most common type of secondary tauopathy. While stabilizing microtubules is a well-established role for tau, tau is also localized at postsynaptic sites and can disrupt synaptic plasticity when knocked out or overexpressed. A major gap in understanding tau functions is identifying the intracellular mechanisms through which tau modulates synaptic function. Here, we found that overexpression of the 0N4R isoform of tau in HEK 293 cells decreased the stability of the activity-regulated cytoskeleton-associated protein (Arc), an immediate early gene that plays a key role in synaptic plasticity, learning and memory. Importantly, tau-induced Arc degradation was found to be isoform-specific in that overexpression of the 0N3R tau isoform had no effect. Tau-dependent reduction of Arc required proteasome activity, yet was independent of Arc ubiquitination. Surprisingly, tau-induced Arc removal required the endophilin-binding domain of Arc. Overexpression of 0N4R tau in primary hippocampal neurons led to Arc instability exclusively in neuronal dendrites, which was coupled to increases in the expression of dendritic and somatic surface GluA1-containing α-amino-3-hydroxy-5-methyl-4-isoxazolepropionic acid (AMPA) receptors. Interestingly, these effects on Arc stability and GluA1 localization were not observed in the commonly studied tau mutant, P301L. Our findings implicate isoform- and domain-specific effects of tau in regulating Arc stability and AMPA receptor targeting, which may in part explain the deficits in synaptic plasticity that are observed in select types of tauopathies.

Introduction

Tauopathies are a diverse group of neurodegenerative disorders predominantly characterized by dementia or degeneration of the motor system (1). A hallmark of tauopathies is the accumulation of tau into insoluble aggregates and filaments which is a major component of neurofibrillary tangles (NFTs) in the brain (2,3). Besides tau pathology, tauopathies may also involve other pathological changes such as amyloid deposition that is observed in Alzheimer's disease (AD) and Down's syndrome (1). In AD, the most common tauopathy, the progress of tau pathology follows a stereotypical pattern in the brain that is highly correlated with the progress of cognitive impairment, which led Braak and Braak to base the staging of AD on the pattern of NFT deposition in the brain (4).

Tau is encoded by the *MAPT* gene on chromosome 17 (5). Its C-terminal region contains 18-residue repeats, which together form the microtubule binding domain (MTBD), which is linked to the N-terminal region through a proline-rich region (6). The *MAPT* gene consists of 16 exons, 11 of which are expressed in the central nervous system (7). In humans, six different isoforms of tau have been reported with differences in alternative mRNA splicing of exons 2, 3 and 10. Alternative splicing of exons 2 and 3 yields 0,1 or 2 N-terminal repeats (0N, 1N and 2N isoforms) while alternative splicing of exon *10* leads to the presence or absence of the R2 domain, which is one of the 4 repeats that bind to microtubules (3R and 4R isoforms) (8). Tau also undergoes several posttranslational modifications including, but not limited to, phosphorylation (9), acetylation (10,11) and ubiquitination (12). During early stages of development, tau is highly phosphorylated and then decreases in the adult brain, to increase again in the aged brain (13-15). In tauopathies, tau becomes hyperphosphorylated, which is thought to increase its propensity to form aggregates and reduce its affinity for microtubules (16).

There are over 50 mutants of the *MAPT* gene that have been identified in several tauopathies (17). Some of these mutations can affect the alternative splicing of *tau* mRNA leading to overproduction of 3R or 4R isoforms and thus pathologically

increasing tau and facilitating its aggregation (18). Other mutations, like the missense P301L mutation found within the 2R region, increase tau phosphorylation, decrease its binding to microtubules resulting in increased levels of free tau, which is thought to promote its aggregation (19). While tau has been well established in its role in stabilizing microtubules (20), more recent studies show that tau has a postsynaptic role that may have effects on synaptic plasticity (21-26).

The activity-regulated cytoskeleton-associated protein (Arc) is an immediate early gene that regulates diverse forms of synaptic plasticity, memory, and learning (27-31). One mechanism through which Arc regulates synaptic plasticity is by promoting the endocytosis of α-amino-3-hydroxy-5-methyl-4-isoxazolepropionic acid (AMPA) receptors through interactions with members of the endocytic machinery; endophilin-2/3, dynamin 2 and AP-2 that predominantly depend on a stretch of amino acids located in N-terminal region referred to as the endophilin binding (EB) domain (30,32,33).

Arc is upregulated during learning in the hippocampus (34) and is rapidly turned over, mainly through its ubiquitination and degradation by the ubiquitin proteasome system (UPS) (35-39). This type of posttranslational destabilization has been identified as a key mechanism for regulating group 1 metabotropic glutamate receptor-mediated long-term depression (mGluR-LTD) and spatial reversal learning (40). Arc is also removed by the autophagic lysosomal pathway (41) and can be degraded by noncanonical neuronal membrane associated proteasomes (42,43). Additionally, Arc undergoes several posttranslational modifications including, but not limited to, phosphorylation (44), sumoylation (45-47), palmitoylation (48), and acetylation (49).

Several studies have examined a role for Arc in AD pathology, mainly through examining the relationship between Arc and β amyloid (50-54). However, there is a gap in understanding the relationship between Arc and tau. Given the role of Arc as a key regulator of synaptic plasticity and the recent implications of tau in regulating synaptic plasticity (21-23), we set out to determine if Arc might be affected by tau pathology. Indeed, we found that overexpression of tau led to reduced Arc stability. Based on this

finding, we tested the role of tau isoforms and mutants in posttranslational regulation of Arc. We found that overexpression of WT-tau but not P301L-tau decreased Arc levels. This reduction was proteasome-dependent and required the R2 region of the tau MTBD. Surprisingly, tau-dependent Arc degradation was not associated with lysosomal degradation or known Arc posttranslational modifications that included ubiquitination, phosphorylation, acetylation, or sumoylation. However, tau-dependent degradation did require the EB domain of Arc. Tau-induced Arc degradation was also found to selectively occur in primary hippocampal dendrites and was associated with increased surface GluA1-containg AMPA receptors in dendrites and abnormal targeting of surface GluA1 to the soma. Our findings highlight a unique role of 0N4R WT-tau in spatially and noncanonically regulating Arc removal, with hints of tau microtubule binding and Arc endocytic targeting in regulating synaptic function.

Results

While evaluating a role for Arc in regulating the release and spread of exosomal tau in HEK 293 cells, we found that overexpression of tau resulted in reduced Arc levels when compared to control conditions (data not shown). Given this surprising finding, we hypothesized that one of the mechanisms through which tau regulates synaptic function is through posttranslational regulation of Arc. To confirm our previous findings, we co-transfected HEK 293 cells with N-terminal myc tagged Arc (myc-Arc) and an increasing amount of GFP-tau (Fig. 1, A-B). Increasing GFP-tau led to a decline in total myc-Arc as demonstrated by immunoblot analysis (Fig. 1B; Kruskal-Wallis, $p=0.0009$, Dunn's post-hoc test 0 vs 1 μg: $p = 0.018$, 0 vs. 1.5 μg: $p = 0.0049$, 0.25 vs 1.5 μg: $p = 0.0301$). P301L is a missense single-point mutation located on the R2 MTBD of tau that substitutes Proline for Leucine, and has been commonly used to model AD pathology (17). Unlike GFP-tau, overexpressing GFP-P301L tau did not have an effect on myc-Arc levels (Fig. 1C; One-way ANOVA, $F (5,18) = 0.3018$, $p = 0.3$).

The Tau-P301S mutation is found to occur in Familial FTD and is used in the PS19 transgenic mouse model to study AD (55). We asked if a mutation at the same P301 site that substitutes Proline for Serine (P301S) (Fig. 1A) would decrease Arc.

Surprisingly, unlike GFP-P301L tau, expression of GFP-P301S tau decreased Arc in a similar manner to GFP-tau (Fig. 1D: One-way ANOVA, $F(5,18) = 10.96$, $p = <0.0001$, Tukey's post-hoc test 0 vs 0.5 μg: $p = 0.0064$, 0 vs. 0.75 μg: $p = 0.0002$, 0 vs. 1: $p = 0.0048$, 0 vs. 1.5 μg: $p = 0.0002$, 0.25 vs. 0.75 μg: $p = 0.0061$, 0.25 vs. 1.5 μg: $p = 0.0085$). Given the location of the P301L mutation within the MTBD R2 region of tau, we next asked if R2 was necessary for the modulation of Arc. Co-transfection of Arc with increasing amounts of the 0N3R tau isoform that lacks the R2 repeat did not decrease Arc (Fig. 1E; one-way ANOVA $F(5,18) = 0.034$, $p = 0.999$) suggesting that R2 of the MTBD is essential for this modulation.

Arc ubiquitination targets Arc to the proteasome for degradation and is a major pathway for Arc removal (35,36,39). We assessed whether the reduction of Arc by tau was dependent on proteasome activity. Cells overexpressing myc-Arc and increasing concentrations of GFP-tau were treated with the proteasome inhibitor MG-132 (Fig. 2A). Unlike the DMSO control condition, myc-Arc levels did not decrease upon MG-132 treatment (Fig. 2B; one-way ANOVA for DMSO control, $F(5,12) = 4.03$, $p = 0.022$, Tukey's post-hoc test 0 vs. 1 μg: $p= 0.046$; one-way ANOVA for MG-132, $F(5,12) = 1.9$, $p = 0.15$), suggesting that the tau-mediated Arc decrease is proteasome dependent.

Studies have shown that Arc can be ubiquitinated by the E3 ligases RNF216, UBE3A and CHIP, which induces its rapid degradation by the proteasome (35,36,38). Since protein ubiquitination dominantly occurs on lysine residues, we tested reported Arc ubiquitination sites for RNF216 and UBE3A on lysines which were mutated to arginine to prevent ubiquitination (K55R/K136R/K268R/K269R/K293R, myc-Arc5KR) (35,36) (Fig. 2C). Surprisingly, co-transfection of myc-Arc 5KR with increasing amounts of GFP-tau still led to a reduction in Arc that was similar in magnitude to myc-ArcWT (Fig. 2D; one-way ANOVA $F = (5,18) = 6.4$, $p = 0.0014$, Tukey's post-hoc 0 vs. 0.5 μg = 0.02, 0 vs 0.75 μg $p = 0.0175$, 0 vs. 1 μg $p = 0.0015$, 0 vs. 1.5 μg $p = 0.0016$). These findings suggested that preventing Arc ubiquitination at these sites does not interfere with tau-mediated Arc reduction. To determine if the tau-mediated decreases in Arc involved

ubiquitination, we measured myc-Arc ubiquitination in the presence of GFP-tau or GFP-P301L tau after treatment with MG-132 to trap Arc ubiquitinated products. While RNF216 robustly increased myc-Arc ubiquitination, this was not observed upon GFP-tau or GFP-P301L tau overexpression (Fig. 2E). To test if Arc could interact with WT-tau, we performed co-immunoprecipitation assays with WT or P301L-tau. While RNF216 efficiently co-immunoprecipitated with Arc, interaction with WT or P301L-tau was not different compared to background control (Fig. 2F). Taken together, these experiments suggest that even though tau modulation of Arc is proteasome dependent, it does not appear to be through a direct interaction with Arc or through enhancing Arc ubiquitination by RNF216 or UBE3A, which indicates that tau might be utilizing noncanonical methods of Arc removal by the proteasome.

One alternative possibility to our MG-132 results could be related to the ability of MG-132 to block late phases of lysosomal degradation (56). Given that Arc is also removed by the autophagy lysosome system in neurons (41), we asked if tau decreases Arc by lysosome-dependent degradation. We treated cells overexpressing myc-Arc and GFP-tau with the lysosome inhibitors Leupeptin and Ammonium Chloride for 6 h before harvest (Fig. 3A) yet still, Arc levels decreased with GFP-tau overexpression in both vehicle and inhibitor-treated conditions (Fig. 3B; Unpaired t-test for vehicle control, $t = 10.6$, $df = 10$, $p < 0.0001$; Unpaired t-test for inhibitors, $t = 5.585$, $df = 10$, $p = 0.0002$). We confirmed inhibition of the lysosomal activity by blotting for markers of autophagic flux – MAP1LC3B (hereafter LC3) and p62/SQSTM1 (57). There was a significant increase in the levels of the autophagosome bound form of LC3 – LC3-II (Figure 3C; unpaired t-test, $t = 12.52$, $df = 22$, $p < 0.0001$) and the autophagosome substrate p62/SQSTM1 (Figure 3C; unpaired t-test, $t = 10.54$, $df = 22$, $p < 0.0001$) in cells treated with lysosome inhibitors as compared to vehicle treated cells. Surprisingly, we did not observe the expected increase in Arc levels as reported previously (data not shown, Unpaired t-test, $t = 0.7087$, $df = 10$, $p = 0.4947$). These findings suggest that tau modulation of Arc is not lysosome dependent.

Given the ability of overexpressed tau to form insoluble aggregates (58,59), we next asked if tau may be precipitating Arc into insoluble aggregates that could not be extracted in the RIPA-soluble fraction. We extracted proteins in the RIPA-insoluble fraction using formic acid, which has been successfully used to extract tau aggregates (60,61). While GFP-tau was detected in the insoluble fraction, Arc was not (Fig. 3D), suggesting that tau-dependent decreases in Arc are not due to its precipitation into insoluble aggregates.

One recent study showed that Arc phosphorylation by GSK3α/β can enhance Arc removal by the proteasome by promoting Arc ubiquitination on K136 (44). We treated cells co-expressing myc-Arc and GFP-tau with the GSK3α/β inhibitor CHIR 98014 (CH98) for 4 h prior to harvest (Fig. 4A). Myc-Arc levels decreased with GFP-tau overexpression in both vehicle and the CH98-treated condition (Fig. 4B; Unpaired t-test for vehicle control, $t = 3.450$, $df = 18$, $p = 0.0029$; unpaired t-test for CH98, $t = 3.417$, $df = 18$, $p = 0.0031$). It was also reported that Arc is phosphorylated on S170, T175, T368, and T380 by GSK3α/β (44) (Fig. 4B). We mutated these phosphorylation sites to generate myc-Arc S170A/T175A, myc-Arc T368, and myc-Arc T380A. However, upon overexpression with GFP-tau (Fig. 4, C-E), all 3 of these myc-Arc phosphorylation mutants were still decreased (Fig. 4, C-E; Unpaired t-test for Arc S170A/T175A, $t = 4.913$, $df = 16$, $p = 0.0002$; Unpaired t-test for Arc T368A, $t = 8.714$, $df = 4$, $p = 0.001$; Unpaired t-test for Arc T380A, $t = 11.59$, $df = 4$, $p = 0.0003$). Together, these experiments demonstrate that tau modulation of Arc is not mediated through GSK3α/β activity or GSK3α/β-dependent Arc phosphorylation.

Given the lack of effects of ubiquitin and phosphorylation modifying sites to mediate Arc removal by tau, we next evaluated regions of Arc that might be necessary for tau-dependent reductions. We used myc-Arc constructs that lack specific domains of Arc; myc-Arc ΔC-terminal (lacking the C-terminal domain), myc-Arc ΔCC (lacking the coiled-coil motif on the N-terminal domain), and myc-Arc ΔEB (lacking the EB domain on the N-terminus) (36) (Fig. 5A). We found that all the tested myc-Arc constructs were

significantly decreased with tau except for the myc-Arc ΔEB (Fig. 5, B-E; Unpaired t-test for WT Arc $t = 8.857$, $df = 10$, $p < 0.0001$; Unpaired t-test for Arc ΔC-terminal $t=6.471$, $df = 10$, $p < 0.0001$; Unpaired t-test for Arc ΔCC $t = 7.076$, $df = 10$, $p < 0.0001$; Unpaired t-test Arc ΔEB $t = 0.2956$, df =1 0, $p = 0.774$). It is worth noting that removal of the coiled-coil domain (myc-Arc ΔCC) reduced the magnitude of tau-induced Arc loss which could indicate a partial role for this domain (Fig. 5D). Cumulatively, these findings show that the EB domain of Arc is essential for its reduction by tau.

The Arc EB domain is a 11 amino acid sequence that is important for targeting Arc to endosomes (32). Recently, Arc was found to be acetylated at K24, K33, K55 and K92 which increases its stability (49). Of these sites, K92 falls within the EB domain (89-100) (Fig. 5A). We hypothesized that tau could be decreasing Arc stability by interfering with its acetylation at K92. To test this hypothesis, we created the acetyl-mimetic myc-Arc K92Q, which increases the stability of Arc (49). However, the myc-Arc K29Q mutant was still reduced with GFP-tau overexpression suggesting that tau does not modulate Arc through interfering with its acetylation at K92 (Fig. 5F; Unpaired t-test $t = 5.54$, $df = 10$, $p = 0.0002$).

To determine if tau altered Arc stability in neurons, GFP-tau and GFP-P301L tau were overexpressed with increasing concentrations in primary hippocampal neurons and endogenous Arc levels were quantified. Td-tomato was used as a cell fill to outline neuronal morphology (Fig. 6A). Interestingly, we found that Arc protein was selectively decreased in dendrites upon GFP-tau overexpression as this decrease was not observed in the soma. Similar to our experiments in HEK293 cells, the GFP-P301L tau had no effect on Arc in neither soma or dendrites (Fig. 6B; one-way ANOVA in dendrites $F (4,88) = 4.4$, $p = 0.0027$, Tukey's post-hoc GFP vs. 2X Tau $p = 0.0042$, GFP vs. 4X Tau $p = 0.013$; one-way ANOVA in soma $F (4,99) = 1.342$, $p = 0.259$). To determine if tau modulation of Arc in hippocampal neurons is proteasome-dependent, primary hippocampal neurons overexpressing GFP-tau were treated with the proteasome inhibitor MG-132 and Arc levels were quantified (Fig. 7A). In Vehicle treated neurons,

Arc was significantly decreased with GFP-tau overexpression but not in MG-132-treated neurons (Fig. 7B; Unpaired t-test DMSO Control in dendrites $t = 2.72$, $df = 27$, $p = 0.011$; Unpaired t-test MG-132 in dendrites $t = 0.3814$, $df = 27$ $p = 0.706$; Unpaired t-test DMSO in soma $t = 1.044$, $df = 27$, $p = 0.306$; Unpaired t-test MG-132 in soma $t = 0.16$, $df = 27$, $p = 0.874$). Our findings support the notion that tau modulation of Arc is selective for dendrites and is proteasome dependent.

Given that Arc interacts with endophilin and dynamin to promote endocytosis of AMPA receptors (28,32), we hypothesized that the tau-mediated decrease of Arc in dendrites would decrease AMPA receptor endocytosis and consequently lead to an increase in surface AMPA receptor levels. To test this, we overexpressed GFP-tau and GFP-P301L tau in primary hippocampal neurons and quantified surface GluA1-containing AMPA receptors (Fig. 8A). GluA1 staining in neurons overexpressing GFP-tau had a smoother appearance, unlike the punctate distribution in neurons overexpressing GFP and GFP-P301L tau. As expected, GFP-tau overexpression led to an increase in surface GluA1; however, this effect was not selective to dendrites, as overexpression also led to an increase of surface GluA1 in the soma (Fig. 8B, Kruskal-Wallis test for dendrites, $p = 0.0458$, Dunn's multiple comparisons test, GFP vs GFP-tau $p = 0.0415$; Kruskal-Wallis test for soma, $p = 0.0034$, Dunn's multiple comparisons test, GFP vs GFP-tau $p = 0.0023$). Cumulatively, these findings suggest that WT but not GFP-P301L tau overexpression disrupts dendritic targeting of GluA1-containing AMPA receptors.

Discussion

Here we show that overexpression of the 0N4R isoform of tau, but not the 0N3R or P301L tau, decreases Arc in HEK293 cells and in the dendrites of primary hippocampal neurons. The reduction of Arc by tau was also found to require the R2 MTBD of tau. Tau modulation of Arc was proteasome-dependent yet occurred independently of Arc ubiquitination. While tau-induced Arc degradation was independent of the numerous known Arc posttranslational modifications, the EB domain of Arc was identified as being necessary for tau-induced Arc degradation. We also show that tau, but not P301L tau,

increased surface GluA1 in both the dendrites and soma in hippocampal neurons, suggesting mistargeting of GluA1 to the soma.

Several studies have shown a role for Arc in AD, mainly through links to amyloid-beta (Aβ). For example, both increases and decreases in Arc in the hippocampus and cortex were reported in several amyloid precursor protein (APP) mouse models (50-53,62-64) and it has been suggested that these changes occur in an age-dependent manner (65,66). Arc levels are also increased in the medial prefrontal cortex of patients with AD (54). On the other hand, a mechanistic relationship between Arc and tau has been relatively understudied. While experience-driven Arc responses were found to be disrupted in the vicinity of plaques in the APP/PS1 model, where neurons in the vicinity of amyloid plaques were less likely to respond, no similar effect was observed in the vicinity of tau NFTs in the Tg4510 mouse overexpressing P301L tau (67,68). A recent study showed that tau elevated Arc1 in a drosophila AD model overexpressing R406W tau, a mutant linked to Frontotemporal dementia, demonstrating a role for Arc1 in neurodegeneration (69). We tested this mutant in HEK293 cells and found that it still led to Arc instability (data not shown). While the conflicting results make it difficult to define a clear role for Arc in AD pathology, this can be attributed to differences in species, the disease models used, the stage of disease development, and the tissue type. Differences in levels of excitability between networks and brain areas can also explain some of the contradictions as Arc levels increase rapidly in excited synapses and upon exposure to learning experiences followed by its removal to return to its basal levels (36,65,70-72).

We show that tau modulation of Arc is proteasome dependent. A major pathway for removal of Arc is through the UPS (35-39). However, creating mutations of characterized Arc ubiquitination sites targeted by the E3 ligases RNF216 and UBE3A (Arc5KR) did not block Arc degradation. Although we did not test for a role of CHIP, an E3 ligase that regulates the ubiquitination of both Arc and tau (38,73), the possibility remains unlikely as we could not detect an enhancement of Arc ubiquitination upon tau overexpression. Moreover, tau modulation of Arc was not dependent on Arc

phosphorylation or lysosomal degradation. In light of these findings, two alternative mechanisms can still be hypothesized. First, recent studies have found that Arc can be assembled into viral-like capsids and released into the extracellular space (74-76). It is possible that tau overexpression may promote the extracellular release of Arc capsids. Second, Arc is a substrate of the 20S neuronal membrane proteasome (NMP), which is proteasome inhibitor sensitive and utilizes a ubiquitin-independent mechanism for degradation of ribosome-associated Arc (42,43). Thus, it is possible that tau could be targeting newly synthesized Arc for removal by the NMP.

We show that the EB domain of Arc is required for its degradation by tau and that 0N3R tau isoform lacking the R2 MTBD did not induce Arc degradation. Structurally, Arc consists of two juxtaposed domains, a positively charged N-terminal domain (NTD) and a negatively charged C-terminal domain (CTD). The NTD has several peptide-binding sites, including the EB and two long helices possibly forming a coiled-coil (77,78). Given our findings requiring the EB of Arc, we investigated the possibility that tau overexpression could be interfering with Arc stability by disrupting the acetylation of Arc at K92 located within this domain (49), but an acetyl mimetic Arc mutant at this site (K92Q) did not prevent the decrease in Arc. Moreover, Arc did not co-immunoprecipitate with tau even when blocking its degradation with the proteasome inhibitor MG-132, suggesting an indirect or transient interaction between these two proteins. Arc binds endophilin, dynamin, and AP-2 to mediate endocytosis of AMPA receptors (32,33). Recent findings show that tau (2N4R) has an extensive network of interactions with proteins that regulate endocytosis, including endophilin, AP-2 and dynamin (26,79). Interestingly, expression of human tau (0N4R) induces de novo assembly of microtubules which interferes with endocytosis through sequestration of dynamin (80). Although we are unable to define a detailed mechanism for the modulation of Arc by tau, our results suggest the involvement of the endocytic machinery, engaged by both Arc (via its EB domain) and tau (via its R2 MTBD), in this process.

Consistent with the observed decrease in Arc specifically in hippocampal dendrites upon tau overexpression, we found that WT tau overexpression also increases surface

levels of GluA1 in the soma of primary hippocampal neurons and in dendrites. Since surface GluA1 was also increased in the soma despite no detected change in Arc in that region, we propose that tau overexpression mistargets GluA1-containing AMPA receptors to the soma due to altered trafficking. The physiological interactions of dendritic tau with synaptic proteins that regulate postsynaptic receptor trafficking and synaptic plasticity have been described (21,26,81-83). Consistent with our findings, tau knockout cortical and hippocampal neurons show significantly lower surface GluA1 compared to wildtype cells (26). Tau interacts with several proteins that regulate AMPA receptor trafficking profiles such as NSF and PICK1 (26,82), and tau knockout neurons show a rapid reduction in the number of GluA2 puncta after NMDA treatment (84). Additionally, tau plays a role in the postsynaptic targeting of the Src kinase Fyn, which regulates the activation of NMDA receptors (21), and consequently affects AMPA receptor trafficking (85). Thus, the observed results could be a net effect of the interaction of tau with several proteins. The sequestration of these proteins could lead to Arc instability. In contrast, we did not observe a change in surface GluA1 with P301L tau overexpression in the soma or dendrites of hippocampal neurons. Hoover et al. reported higher levels of P301L tau in postsynaptic density proteins isolated from rTg4510 mice overexpressing P301L tau compared to those isolated from rTg21221 mice overexpressing WT tau (0N4R). rTgP301L neurons showed lower synaptic GluA1 levels compared to neurons from rTgWT mice at DIV 21-35 (86). In our study, WT and P301L tau are acutely overexpressed, and neurons were fixed at DIV 12-14 and thus our findings may model an earlier stage of tau pathology. Additionally, the insertion of the transgene *MAPT P301L* in the Tg4510 model disrupts the *fibroblast growth factor 14* (*Fgf14*) gene, which has been shown to contribute to the neurodegeneration observed in the mouse model, which may have inadvertently resulted in off target effects on surface GluA1 (87,88).

While different tau isoforms and mutants are used interchangeably to model AD and other tauopathies, our study adds to the growing body of literature that emphasizes the differences in protein interactions between tau isoforms and mutants, which provides further support of their unique roles in the cell and their differential contributions to

disease pathogenesis (79,89-92). The six isoforms of tau are also differentially expressed throughout development, with the ratio of 3R to 4R tau in the adult human brain roughly equal to one (8). Tau isoforms further have distinct biochemical properties such as different propensities for aggregation, with those containing 4R assembling 2.5 to 3 times faster compared to 3R isoforms (93). In AD, NFTs contain all six isoforms, while in other tauopathies, tangles may predominantly have 3R or 4R tau (94). On the other hand, the majority of *MAPT* mutations, including P301L, are associated with FTD. However, P301L as well as other *MAPT* mutations have been commonly used to model AD in vivo and in vitro despite their distinct physical properties (95). The genetically matched rT1 model overexpressing WT 0N4R human tau and rT2 model overexpressing P301L-tau also show differences in tau phosphorylation and stability at different developmental stages compared to mice overexpressing P301L-tau (96).

Our study demonstrates a posttranslational role for tau in regulating Arc, a key mediator of synaptic plasticity and opens up possibilities of identifying new pathways for removing Arc. Our findings also show that the endocytic targeting of Arc is important for tau-induced instability. Requirements of the MTBD of tau in Arc stability further emphasize a critical role for this region in regulating synaptic proteins and highlights the importance of distinctions in downstream signaling mechanisms activated by different tau isoforms and mutants involved in neurodegenerative disease.

Experimental Procedures

Animals

All animal care and use were carried out in accordance with the National Institutes of Health Guidelines for the Use of Animals using approved protocols by the Georgia State University Institutional Animal Care and Use Committee.

HEK293 cell line cultures and transfections

HEK293 cells were generously provided by Dr. Jun Yin (Georgia State University). Cells were maintained in Dulbecco’s Modified Eagle Medium (DMEM; Corning # 10013CV) with 10% FBS and 1% penicillin-streptomycin (ThermoFisher). Cells were transfected at

60-70% confluency with Lipofectamine 3000 (ThermoFisher) according to the manufacturer instructions. Culture media was exchanged 4 hr post-transfection to remove transfection material and cells were harvested 48 h later. For proteasome inhibition experiments, cells were treated with 10 μM MG-132 (sigma # 474790) for 4 hr before harvesting. For lysosome inhibition experiments, cells were treated with 50 μM leupeptin (Sigma # L2884) and 10 mM NH_4Cl (Sigma # A9434) as described in (41) for 6 hr before harvesting. For GSK3α/β inhibition, cultures were treated with 1-2 μM CHIR 98014 (Tocris #6695) as described in (44) for 4 hr before harvesting.
Plasmids used for transfection include the following: pcDNA 3.1, pEGFP-C3 (Clontech), pCMV-Td tomato, pRK5-myc-Arc (generously provided by Dr. Paul Worley, Johns Hopkins University), pRK5-myc-Arc5KR, pRK5-myc-Arc S170A/T175A, pRK5-myc-Arc T368A, pRK5-myc-Arc T380A, pRK5-myc-Arc K92Q, pRK5-myc-Arc Δ C-terminal, pRK5-myc-Arc Δ CC, pRK5-myc-Arc Δ EB (36), pEGFP-WT Tau (Addgene), pEGFP-P301L tau (Addgene). pcDNA 5/TO-0N3R Tau was generously provided by Dr. Todd Cohen, University of North Carolina (97).

Cloning

QuickChange™ Site-directed mutagenesis (SDM) was used to generate the mutants pRK5-myc-Arc S170A/T175A, pRK5-myc-Arc T368A, pRK5-myc-Arc T380A, pRK5-myc-Arc K92Q from the pRK5-myc-Arc backbone. pEGFP-P301S Tau was generated from the pEGFP- WT Tau backbone. Primers used were as follows:
S170A/T175A For.: 5'-GGCTACGACTACACTGTTGCCCCCTATGCCATCGCCCCGCCACCTGCCGCAGGA-3', S170A/T175A Rev.: 5'-TCCTGCGGCAGGTGGCGGGGCGATGGCATAGGGGGCAACAGTGTAGTCGTAGC-3'; T368A For.: 5'-GGCAGCTGAGCCTTCTGTCGCCCCTCTGCCCACAGAGGATG-3', T368A Rev.: 5'-CATCCTCTGTGGGCAGAGGGGCGACAGAAGGCTCAGCTGCC-3', P301S For.: 5'-AAAGGATAATATCAAACACGTCTCGGGAGGCGGCAGTGTGCAAATAG-3',

P301S Rev.: 5'-CTATTTGCACACTGCCGCCTCCCGAGACGTGTTTGATATTATCCTTT-3';
K92Q For.: 5'-GGAAGAAGTCCATCCAGGCCTGTCTCTGC-3',
K92Q Rev.: 5'-GCAGAGACAGGCCTGGATGGACTTCTTCC-3'.
The T380A mutant was generated using the overlap extension method as previously described in (98) with the flanking primers 5'-GAAGTCGACCCCGGGAATGGAGCTGGA-3', 5' GAAGGATCCTTACTTACTTAGCGGCCG 3' and Fwd.: 5'-GATGAGACTGGGGCACTCGCCCCTGCTCTTACCAGCGAG-3', Rev.: 5'-CTCGCTGGTAAGAGCAGGGGCGAGTGCCCCAGTCTCATC-3' at the site of the mutation. BamHI and SalI restriction enzymes (New England Biolabs) were used to subclone the mutated fragment into the pRK5-myc-Arc backbone.

Western Blotting

HEK293 Cells were harvested and then cell pellets were lysed on ice in radioimmunoprecipitation assay (RIPA) buffer (150 mM NaCl, 50 mM Tris-HCl, 1% v/v Nonidet P-40, 0.05% sodium deoxycholate, 0.01% SDS) with 1 mM DTT and protease inhibitors (0.1 mM PMSF, 1 μM leupeptin, 0.15 μM aprotinin). Lysates were centrifuged at 13,000 rpm for 20 min at 4°C to precipitate insoluble extracts. Protein concentrations were measured using the Pierce 660 assay (ThermoFisher). To extract insoluble proteins, the precipitated pellet was resuspended in RIPA buffer then centrifuged at 13,000 rpm for 20 min at 4°C then resuspended in 70% formic acid and vortexed for 2 min. The samples were centrifuged at 13,000 rpm for 20 min at 4°C, the pellet discarded and 20 volumes of neutralization buffer (1M Tris Base, 0.5 M Na_2PO_4 with protease and phosphatase inhibitors) were added to the supernatant.
Proteins were separated by SDS-PAGE then transferred to nitrocellulose membrane at 4°C (0.45 μm pore size, Bio-Rad). Membranes were blocked overnight at 4° in Intercept tris-buffered saline (TBS) blocking buffer (LI-COR) then incubated in primary antibodies in 1:1 blocking buffer to 1% Tween-20 in TBS (TBST) with 0.02% NaN_3 overnight at 4°C. Membranes were washed 3 times with double distilled water for 5 min, and

secondary antibodies in 1:1 blocking buffer to TBST 0.1% SDS were added to the membranes for 1 hr at room temperature, then washed 2 times with TBST and 1 time with double distilled water for 5 min.

Primary antibodies used: mouse anti-myc (Santa Cruz #sc-40) at 1:1000, rabbit anti-GFP (Novus Biologicals # NB600-308) at 1:1000, mouse anti-β Actin (Genetex #GTX629630) at 1:3000, mouse anti-Tau-1 (Fisher #MAB3420MI) at 1:1000, mouse anti-Tubulin (Genetex # GT114) at 1:1000, mouse anti-Ubiquitin (Sigma # U5379) at 1:500, rabbit anti-LC3 (Novus biologicals #NB100-2220) at 1:500, rabbit anti-p62 (Proteintech #18420-1-AP) at 1:1000.

Secondary antibodies used: IRDye goat anti-mouse 680RD (LI-COR #926-68070) at 1:20,000, IRDye donkey anti-rabbit 680RD (LI-COR # 925-68073) at 1:20,000, IRDye donkey anti-mouse 800CW (LI-COR #926-32212) at 1:15,000, IRDye goat anti-rabbit 800CW (LI-COR # 926-32211) at 1:15,000.

Western blot membranes were scanned using the LI-COR Odyssey CLx scanner (low scan quality, 163 µm scan resolution, auto channel intensities). Images were analyzed using ImageJ software (NIH) with the Gel Analysis tool or Image studio Lite software (Li-COR Biosciences). To adjust high background, the Subtract Background tool in FIJI was used on the whole channel with a rolling ball radius of 20-50 pixels.

Co-Immunoprecipitation

Transfected cells were lysed in IP buffer (20 mM Tris-HCl, 3 mM EDTA, 3 mM EGTA, 150 mM NaCl, 1% Triton X-100, pH 7.4) with 1 mM DTT, protease and phosphatase inhibitors (0.1 mM PMSF, 1 µM leupeptin, 0.15 µM aprotinin, and 1:2000 Halt phosphatase inhibitor cocktail; ThermoFisher #78420). Lysates were centrifuged at 13,000 rpm for 20 min at 4°C to precipitate insoluble extracts. Protein concentration was determined using the Pierce assay 660 assay (ThermoFisher). 1 mg of protein was used for each condition and brought up to a total volume of 1 ml in IP buffer. Beads (Protein A/G PLUS-Agarose; Santa Cruz #sc-2003) were pre-equilibrated in IP buffer

with inhibitors. Protein samples were incubated with 2.5 µg/sample of the primary antibody (Goat anti-myc (bethyl #A190-104A) or mouse anti-myc (Santa Cruz #SC-40)) and left to tumble for 1 hr at 4°C, then equal volume of beads suspension was added per sample and left to tumble overnight. Samples were centrifuged for 45 seconds at 13,000 rpm to pellet the beads. The supernatant was discarded, and beads were washed 3 times for 5 min with IP buffer before adding 2X SDS sample buffer (4% SDS, 20% glycerol, 0.2% bromophenol blue, 3% DTT, 0.1 M Tris-HCl, 1:1000 β-mercaptoethanol, pH 6.8) and heating to 45°C for 5 min. Proteins were then separated using SDS-PAGE as described above.
For the ubiquitination assay, the same protocol was followed except that RIPA buffer was used instead of IP buffer.

Primary Hippocampal Neuronal Cultures

Primary hippocampal neurons of mixed sex were isolated from P0-1 mice as previously described (40) and cultured on poly-d-lysine-coated coverslips (1 mg/ml) in 24-well plates at a density of 75,000 cells/well. Cultures were maintained in neuronal feeding media: Neurobasal media (ThermoFisher) containing 1% GlutaMAX (ThermoFisher), 2% B-27 (ThermoFisher), 4.8 µg/mL 5-Fluoro-2'-deoxyuridine (Sigma), and 0.2 μg/mL Gentamicin (Sigma). On day *in vitro* (DIV) 6, half the media was replaced with prewarmed fresh neuronal feeding media. Cultures were transfected with Lipofectamine 2000 (ThermoFisher) on DIV 9-12 as described in (36) with equal amount of cDNA transfected into all conditions. For proteasome inhibition experiments, cultures were treated with 0.5 μM tetrodotoxin citrate (TTX; Tocris #1069) and 10 μM MG132 for 4 hr before they were fixed.

Immunocytochemistry

48 h after transfection, cultures were treated with 2 μM TTX for 4 h then fixed for 20 min at 4°C with 4% Sucrose/4% paraformaldehyde. Neurons were permeabilized with 0.2 % Saponin for 15 min then blocked in 10 % normal horse serum (NHS) in PBS for 1 hr at 37°C. Permeabilization was skipped for surface labelling. Neurons were then incubated

overnight in primary antibody in 3% NHS, then washed and incubated in secondary antibody at 1:1,000 and DAPI at 1:2,000 in 3% NHS for 1 h in the dark at room temperature. Coverslips were washed with phosphate buffer saline (PBS) then mounted onto slides with Fluorogel (GeneTex).
Primary Antibodies used: rabbit anti-Arc (synaptic systems #156003) at 1:500, mouse anti-GluA1 (Millipore MAB2263) at 1:150.
Secondary Antibodies used: Donkey anti-rabbit AlexaFluor 647 (ThermoFisher #A31573), Goat anti-mouse AlexaFluor 647 (ThermoFisher #A21240)

Image Acquisition and Analysis

For primary hippocampal neurons, coverslips were imaged on a Zeiss LSM 700 confocal microscope under 40X (Arc experiments NA 1.4, Zeiss #420762-9900) or 63X (NA 1.4, Zeiss #420782-9900-000, GluA1 experiments) immersion lens. 12-step raw z-stack images were acquired with step size 0.42 μm. Acquisition parameters were kept constant between different conditions within the same experiment and samples were interleaved during imaging. Images were analyzed using ImageJ software (NIH). Regions of interest were manually outlined guided by the neuron morphology visualized by the Td-tomato cell fill, and integrated density values were quantified for Arc and GluA1 in the initial 20 μm of apical dendrites.

Experimental design and statistical analysis

All experiments follow a between-subjects design. Statistical analysis was conducted using GraphPad prism as described in the text for each experiment. Non-parametric tests are used when the criteria for using parametric tests are not met. Data is represented as mean ± SEM with statistical significance set at 95%.

Data Availability

All data and materials are available upon request from the lead contact author.

Acknowledgments

We would like to thank the Dr. Jun Yin (Georgia state University), Dr. Todd Cohen (University of North Carolina-Chapel Hill) and Dr. Paul Worley (John Hopkins University) for providing reagents, and Mabb lab members for feedback on experiments. We would also like to thank the Neuroscience Institute confocal core staff and GSU Division of Animal Resources.

Author Contributions

DWY designed the study, performed experiments, and wrote the manuscript. AS confirmed lysosomal inhibition and edited the mabuscript, and ZDA prepared primary neuronal cultures. TYN contributed to experiment design and edited the manuscript. AMM supervised and designed the study, edited the manuscript, and contributed to manuscript writing.

Funding and Additional Information

This study was funded by the Brain & Behavior Research Foundation NARSAD Young Investigator Award (Grant 28549), NIH/NINDS grant 1R21NS116760 and NSF CAREER Award 2047700 to AMM, and NIH/NIGMS grant GM119571 to TYN. DWY was funded by a Georgia State University Second Century Initiative Neurogenomics Fellowship, Georgia State University Molecular Basis of Disease Fellowship, and Kenneth W. and Georganne F. Honeycutt Fellowship.

Conflict of Interest

The authors declare no competing interests.

References

1. Williams, D. R. (2006) Tauopathies: classification and clinical update on neurodegenerative diseases associated with microtubule-associated protein tau. *Intern Med J* **36**, 652-660
2. Kosik, K. S., Joachim, C. L., and Selkoe, D. J. (1986) Microtubule-associated protein tau (tau) is a major antigenic component of paired helical filaments in Alzheimer disease. *Proc Natl Acad Sci U S A* **83**, 4044-4048
3. Wood, J. G., Mirra, S. S., Pollock, N. J., and Binder, L. I. (1986) Neurofibrillary tangles of Alzheimer disease share antigenic determinants with the axonal microtubule-associated protein tau (tau). *Proc Natl Acad Sci U S A* **83**, 4040-4043
4. Braak, H., and Braak, E. (1995) Staging of Alzheimer's disease-related neurofibrillary changes. *Neurobiol Aging* **16**, 271-278; discussion 278-284
5. Andreadis, A., Brown, W. M., and Kosik, K. S. (1992) Structure and novel exons of the human tau gene. *Biochemistry* **31**, 10626-10633
6. Wolfe, M. S. (2009) Tau mutations in neurodegenerative diseases. *J Biol Chem* **284**, 6021-6025
7. Goedert, M., Wischik, C. M., Crowther, R. A., Walker, J. E., and Klug, A. (1988) Cloning and sequencing of the cDNA encoding a core protein of the paired helical filament of Alzheimer disease: identification as the microtubule-associated protein tau. *Proc Natl Acad Sci U S A* **85**, 4051-4055
8. Goedert, M., Spillantini, M. G., Jakes, R., Rutherford, D., and Crowther, R. A. (1989) Multiple isoforms of human microtubule-associated protein tau: sequences and localization in neurofibrillary tangles of Alzheimer's disease. *Neuron* **3**, 519-526
9. Reynolds, C. H., Betts, J. C., Blackstock, W. P., Nebreda, A. R., and Anderton, B. H. (2000) Phosphorylation sites on tau identified by nanoelectrospray mass spectrometry: differences in vitro between the mitogen-activated protein kinases ERK2, c-Jun N-terminal kinase and P38, and glycogen synthase kinase-3beta. *J Neurochem* **74**, 1587-1595

10. Min, S. W., Cho, S. H., Zhou, Y., Schroeder, S., Haroutunian, V., Seeley, W. W., Huang, E. J., Shen, Y., Masliah, E., Mukherjee, C., Meyers, D., Cole, P. A., Ott, M., and Gan, L. (2010) Acetylation of tau inhibits its degradation and contributes to tauopathy. *Neuron* **67**, 953-966
11. Cohen, T. J., Guo, J. L., Hurtado, D. E., Kwong, L. K., Mills, I. P., Trojanowski, J. Q., and Lee, V. M. (2011) The acetylation of tau inhibits its function and promotes pathological tau aggregation. *Nat Commun* **2**, 252
12. Shimura, H., Schwartz, D., Gygi, S. P., and Kosik, K. S. (2004) CHIP-Hsc70 complex ubiquitinates phosphorylated tau and enhances cell survival. *J Biol Chem* **279**, 4869-4876
13. Harrison, T. M., La Joie, R., Maass, A., Baker, S. L., Swinnerton, K., Fenton, L., Mellinger, T. J., Edwards, L., Pham, J., Miller, B. L., Rabinovici, G. D., and Jagust, W. J. (2019) Longitudinal tau accumulation and atrophy in aging and alzheimer disease. *Ann Neurol* **85**, 229-240
14. Torres, A. K., Rivera, B. I., Polanco, C. M., Jara, C., and Tapia-Rojas, C. (2022) Phosphorylated tau as a toxic agent in synaptic mitochondria: implications in aging and Alzheimer's disease. *Neural Regen Res* **17**, 1645-1651
15. Tuerde, D., Kimura, T., Miyasaka, T., Furusawa, K., Shimozawa, A., Hasegawa, M., Ando, K., and Hisanaga, S. I. (2018) Isoform-independent and -dependent phosphorylation of microtubule-associated protein tau in mouse brain during postnatal development. *J Biol Chem* **293**, 1781-1793
16. Wang, Y., and Mandelkow, E. (2016) Tau in physiology and pathology. *Nat Rev Neurosci* **17**, 5-21
17. Strang, K. H., Golde, T. E., and Giasson, B. I. (2019) MAPT mutations, tauopathy, and mechanisms of neurodegeneration. *Lab Invest* **99**, 912-928
18. D'Souza, I., and Schellenberg, G. D. (2005) Regulation of tau isoform expression and dementia. *Biochim Biophys Acta* **1739**, 104-115
19. Hutton, M., Lendon, C. L., Rizzu, P., Baker, M., Froelich, S., Houlden, H., Pickering-Brown, S., Chakraverty, S., Isaacs, A., Grover, A., Hackett, J., Adamson, J., Lincoln, S., Dickson, D., Davies, P., Petersen, R. C., Stevens, M., de Graaff, E., Wauters, E., van Baren, J., Hillebrand, M., Joosse, M., Kwon, J.

M., Nowotny, P., Che, L. K., Norton, J., Morris, J. C., Reed, L. A., Trojanowski, J., Basun, H., Lannfelt, L., Neystat, M., Fahn, S., Dark, F., Tannenberg, T., Dodd, P. R., Hayward, N., Kwok, J. B., Schofield, P. R., Andreadis, A., Snowden, J., Craufurd, D., Neary, D., Owen, F., Oostra, B. A., Hardy, J., Goate, A., van Swieten, J., Mann, D., Lynch, T., and Heutink, P. (1998) Association of missense and 5'-splice-site mutations in tau with the inherited dementia FTDP-17. *Nature* **393**, 702-705

20. Drechsel, D. N., Hyman, A. A., Cobb, M. H., and Kirschner, M. W. (1992) Modulation of the dynamic instability of tubulin assembly by the microtubule-associated protein tau. *Mol Biol Cell* **3**, 1141-1154
21. Ittner, L. M., Ke, Y. D., Delerue, F., Bi, M., Gladbach, A., van Eersel, J., Wolfing, H., Chieng, B. C., Christie, M. J., Napier, I. A., Eckert, A., Staufenbiel, M., Hardeman, E., and Gotz, J. (2010) Dendritic function of tau mediates amyloid-beta toxicity in Alzheimer's disease mouse models. *Cell* **142**, 387-397
22. Holth, J. K., Bomben, V. C., Reed, J. G., Inoue, T., Younkin, L., Younkin, S. G., Pautler, R. G., Botas, J., and Noebels, J. L. (2013) Tau loss attenuates neuronal network hyperexcitability in mouse and Drosophila genetic models of epilepsy. *J Neurosci* **33**, 1651-1659
23. Roberson, E. D., Scearce-Levie, K., Palop, J. J., Yan, F., Cheng, I. H., Wu, T., Gerstein, H., Yu, G. Q., and Mucke, L. (2007) Reducing endogenous tau ameliorates amyloid beta-induced deficits in an Alzheimer's disease mouse model. *Science* **316**, 750-754
24. Biundo, F., d'Abramo, C., Tambini, M. D., Zhang, H., Del Prete, D., Vitale, F., Giliberto, L., Arancio, O., and D'Adamio, L. (2017) Abolishing Tau cleavage by caspases at Aspartate(421) causes memory/synaptic plasticity deficits and pre-pathological Tau alterations. *Transl Psychiatry* **7**, e1198
25. Biundo, F., Del Prete, D., Zhang, H., Arancio, O., and D'Adamio, L. (2018) A role for tau in learning, memory and synaptic plasticity. *Sci Rep* **8**, 3184
26. Prikas, E., Paric, E., Asih, P. R., Stefanoska, K., Stefen, H., Fath, T., Poljak, A., and Ittner, A. (2022) Tau target identification reveals NSF-dependent effects on AMPA receptor trafficking and memory formation. *EMBO J* **41**, e10242

27. Waung, M. W., Pfeiffer, B. E., Nosyreva, E. D., Ronesi, J. A., and Huber, K. M. (2008) Rapid translation of Arc/Arg3.1 selectively mediates mGluR-dependent LTD through persistent increases in AMPAR endocytosis rate. *Neuron* **59**, 84-97
28. Rial Verde, E. M., Lee-Osbourne, J., Worley, P. F., Malinow, R., and Cline, H. T. (2006) Increased expression of the immediate-early gene arc/arg3.1 reduces AMPA receptor-mediated synaptic transmission. *Neuron* **52**, 461-474
29. Messaoudi, E., Kanhema, T., Soule, J., Tiron, A., Dagyte, G., da Silva, B., and Bramham, C. R. (2007) Sustained Arc/Arg3.1 synthesis controls long-term potentiation consolidation through regulation of local actin polymerization in the dentate gyrus in vivo. *J Neurosci* **27**, 10445-10455
30. Shepherd, J. D., Rumbaugh, G., Wu, J., Chowdhury, S., Plath, N., Kuhl, D., Huganir, R. L., and Worley, P. F. (2006) Arc/Arg3.1 mediates homeostatic synaptic scaling of AMPA receptors. *Neuron* **52**, 475-484
31. Okuno, H., Akashi, K., Ishii, Y., Yagishita-Kyo, N., Suzuki, K., Nonaka, M., Kawashima, T., Fujii, H., Takemoto-Kimura, S., Abe, M., Natsume, R., Chowdhury, S., Sakimura, K., Worley, P. F., and Bito, H. (2012) Inverse synaptic tagging of inactive synapses via dynamic interaction of Arc/Arg3.1 with CaMKIIbeta. *Cell* **149**, 886-898
32. Chowdhury, S., Shepherd, J. D., Okuno, H., Lyford, G., Petralia, R. S., Plath, N., Kuhl, D., Huganir, R. L., and Worley, P. F. (2006) Arc/Arg3.1 interacts with the endocytic machinery to regulate AMPA receptor trafficking. *Neuron* **52**, 445-459
33. DaSilva, L. L., Wall, M. J., L, P. d. A., Wauters, S. C., Januario, Y. C., Muller, J., and Correa, S. A. (2016) Activity-Regulated Cytoskeleton-Associated Protein Controls AMPAR Endocytosis through a Direct Interaction with Clathrin-Adaptor Protein 2. *eNeuro* **3**
34. Guzowski, J. F., McNaughton, B. L., Barnes, C. A., and Worley, P. F. (1999) Environment-specific expression of the immediate-early gene Arc in hippocampal neuronal ensembles. *Nat Neurosci* **2**, 1120-1124
35. Greer, P. L., Hanayama, R., Bloodgood, B. L., Mardinly, A. R., Lipton, D. M., Flavell, S. W., Kim, T. K., Griffith, E. C., Waldon, Z., Maehr, R., Ploegh, H. L., Chowdhury, S., Worley, P. F., Steen, J., and Greenberg, M. E. (2010) The

Angelman Syndrome protein Ube3A regulates synapse development by ubiquitinating arc. *Cell* **140**, 704-716

36. Mabb, A. M., Je, H. S., Wall, M. J., Robinson, C. G., Larsen, R. S., Qiang, Y., Correa, S. A., and Ehlers, M. D. (2014) Triad3A regulates synaptic strength by ubiquitination of Arc. *Neuron* **82**, 1299-1316
37. Mabb, A. M., and Ehlers, M. D. (2018) Arc ubiquitination in synaptic plasticity. *Semin Cell Dev Biol* **77**, 10-16
38. Liu, Y., Sun, Y., Huang, Y., Cheng, K., Xu, Y., Tian, Q., and Zhang, S. (2021) CHIP promotes Wnt signaling and regulates Arc stability by recruiting and polyubiquitinating LEF1 or Arc. *Cell Death Discov* **7**, 5
39. Rao, V. R., Pintchovski, S. A., Chin, J., Peebles, C. L., Mitra, S., and Finkbeiner, S. (2006) AMPA receptors regulate transcription of the plasticity-related immediate-early gene Arc. *Nat Neurosci* **9**, 887-895
40. Wall, M. J., Collins, D. R., Chery, S. L., Allen, Z. D., Pastuzyn, E. D., George, A. J., Nikolova, V. D., Moy, S. S., Philpot, B. D., Shepherd, J. D., Muller, J., Ehlers, M. D., Mabb, A. M., and Correa, S. A. L. (2018) The Temporal Dynamics of Arc Expression Regulate Cognitive Flexibility. *Neuron* **98**, 1124-1132 e1127
41. Yan, J., Porch, M. W., Court-Vazquez, B., Bennett, M. V. L., and Zukin, R. S. (2018) Activation of autophagy rescues synaptic and cognitive deficits in fragile X mice. *Proc Natl Acad Sci U S A* **115**, E9707-E9716
42. Ramachandran, K. V., Fu, J. M., Schaffer, T. B., Na, C. H., Delannoy, M., and Margolis, S. S. (2018) Activity-Dependent Degradation of the Nascentome by the Neuronal Membrane Proteasome. *Mol Cell* **71**, 169-177 e166
43. Ramachandran, K. V., and Margolis, S. S. (2017) A mammalian nervous-system-specific plasma membrane proteasome complex that modulates neuronal function. *Nat Struct Mol Biol* **24**, 419-430
44. Gozdz, A., Nikolaienko, O., Urbanska, M., Cymerman, I. A., Sitkiewicz, E., Blazejczyk, M., Dadlez, M., Bramham, C. R., and Jaworski, J. (2017) GSK3alpha and GSK3beta Phosphorylate Arc and Regulate its Degradation. *Front Mol Neurosci* **10**, 192

45. Nair, R. R., Patil, S., Tiron, A., Kanhema, T., Panja, D., Schiro, L., Parobczak, K., Wilczynski, G., and Bramham, C. R. (2017) Dynamic Arc SUMOylation and Selective Interaction with F-Actin-Binding Protein Drebrin A in LTP Consolidation In Vivo. *Front Synaptic Neurosci* **9**, 8
46. Bramham, C. R., Alme, M. N., Bittins, M., Kuipers, S. D., Nair, R. R., Pai, B., Panja, D., Schubert, M., Soule, J., Tiron, A., and Wibrand, K. (2010) The Arc of synaptic memory. *Exp Brain Res* **200**, 125-140
47. Craig, T. J., Jaafari, N., Petrovic, M. M., Jacobs, S. C., Rubin, P. P., Mellor, J. R., and Henley, J. M. (2012) Homeostatic synaptic scaling is regulated by protein SUMOylation. *J Biol Chem* **287**, 22781-22788
48. Barylko, B., Wilkerson, J. R., Cavalier, S. H., Binns, D. D., James, N. G., Jameson, D. M., Huber, K. M., and Albanesi, J. P. (2018) Palmitoylation and Membrane Binding of Arc/Arg3.1: A Potential Role in Synaptic Depression. *Biochemistry* **57**, 520-524
49. Lalonde, J., Reis, S. A., Sivakumaran, S., Holland, C. S., Wesseling, H., Sauld, J. F., Alural, B., Zhao, W. N., Steen, J. A., and Haggarty, S. J. (2017) Chemogenomic analysis reveals key role for lysine acetylation in regulating Arc stability. *Nat Commun* **8**, 1659
50. Wegenast-Braun, B. M., Fulgencio Maisch, A., Eicke, D., Radde, R., Herzig, M. C., Staufenbiel, M., Jucker, M., and Calhoun, M. E. (2009) Independent effects of intra- and extracellular Abeta on learning-related gene expression. *Am J Pathol* **175**, 271-282
51. Dickey, C. A., Gordon, M. N., Mason, J. E., Wilson, N. J., Diamond, D. M., Guzowski, J. F., and Morgan, D. (2004) Amyloid suppresses induction of genes critical for memory consolidation in APP + PS1 transgenic mice. *J Neurochem* **88**, 434-442
52. Dickey, C. A., Loring, J. F., Montgomery, J., Gordon, M. N., Eastman, P. S., and Morgan, D. (2003) Selectively reduced expression of synaptic plasticity-related genes in amyloid precursor protein + presenilin-1 transgenic mice. *J Neurosci* **23**, 5219-5226

53. Perez-Cruz, C., Nolte, M. W., van Gaalen, M. M., Rustay, N. R., Termont, A., Tanghe, A., Kirchhoff, F., and Ebert, U. (2011) Reduced spine density in specific regions of CA1 pyramidal neurons in two transgenic mouse models of Alzheimer's disease. *J Neurosci* **31**, 3926-3934
54. Wu, J., Petralia, R. S., Kurushima, H., Patel, H., Jung, M. Y., Volk, L., Chowdhury, S., Shepherd, J. D., Dehoff, M., Li, Y., Kuhl, D., Huganir, R. L., Price, D. L., Scannevin, R., Troncoso, J. C., Wong, P. C., and Worley, P. F. (2011) Arc/Arg3.1 regulates an endosomal pathway essential for activity-dependent beta-amyloid generation. *Cell* **147**, 615-628
55. Yoshiyama, Y., Higuchi, M., Zhang, B., Huang, S. M., Iwata, N., Saido, T. C., Maeda, J., Suhara, T., Trojanowski, J. Q., and Lee, V. M. (2007) Synapse loss and microglial activation precede tangles in a P301S tauopathy mouse model. *Neuron* **53**, 337-351
56. van Kerkhof, P., Alves dos Santos, C. M., Sachse, M., Klumperman, J., Bu, G., and Strous, G. J. (2001) Proteasome inhibitors block a late step in lysosomal transport of selected membrane but not soluble proteins. *Mol Biol Cell* **12**, 2556-2566
57. Shroff, A., and Nazarko, T. Y. (2022) SQSTM1, lipid droplets and current state of their lipophagy affairs. *Autophagy*, 1-4
58. Lippens, G., Sillen, A., Landrieu, I., Amniai, L., Sibille, N., Barbier, P., Leroy, A., Hanoulle, X., and Wieruszeski, J. M. (2007) Tau aggregation in Alzheimer's disease: what role for phosphorylation? *Prion* **1**, 21-25
59. Ackmann, M., Wiech, H., and Mandelkow, E. (2000) Nonsaturable binding indicates clustering of tau on the microtubule surface in a paired helical filament-like conformation. *J Biol Chem* **275**, 30335-30343
60. Ishihara, T., Higuchi, M., Zhang, B., Yoshiyama, Y., Hong, M., Trojanowski, J. Q., and Lee, V. M. (2001) Attenuated neurodegenerative disease phenotype in tau transgenic mouse lacking neurofilaments. *J Neurosci* **21**, 6026-6035
61. Dou, F., Netzer, W. J., Tanemura, K., Li, F., Hartl, F. U., Takashima, A., Gouras, G. K., Greengard, P., and Xu, H. (2003) Chaperones increase association of tau protein with microtubules. *Proc Natl Acad Sci U S A* **100**, 721-726

62. Palop, J. J., Chin, J., Bien-Ly, N., Massaro, C., Yeung, B. Z., Yu, G. Q., and Mucke, L. (2005) Vulnerability of dentate granule cells to disruption of arc expression in human amyloid precursor protein transgenic mice. *J Neurosci* **25**, 9686-9693

63. Parra-Damas, A., Valero, J., Chen, M., Espana, J., Martin, E., Ferrer, I., Rodriguez-Alvarez, J., and Saura, C. A. (2014) Crtc1 activates a transcriptional program deregulated at early Alzheimer's disease-related stages. *J Neurosci* **34**, 5776-5787

64. Xu, C., Huang, H., Zhang, M., Zhang, P., Li, Z., Liu, X., and Fang, M. (2022) Methyltransferase-Like 3 Rescues the Amyloid-beta protein-Induced Reduction of Activity-Regulated Cytoskeleton Associated Protein Expression via YTHDF1-Dependent N6-Methyladenosine Modification. *Front Aging Neurosci* **14**, 890134

65. Privitera, L., Hogg, E. L., Lopes, M., Domingos, L. B., Gaestel, M., Muller, J., Wall, M. J., and Correa, S. A. L. (2022) The MK2 cascade mediates transient alteration in mGluR-LTD and spatial learning in a murine model of Alzheimer's disease. *Aging Cell* **21**, e13717

66. Naert, G., and Rivest, S. (2012) Age-related changes in synaptic markers and monocyte subsets link the cognitive decline of APP(Swe)/PS1 mice. *Front Cell Neurosci* **6**, 51

67. Rudinskiy, N., Hawkes, J. M., Betensky, R. A., Eguchi, M., Yamaguchi, S., Spires-Jones, T. L., and Hyman, B. T. (2012) Orchestrated experience-driven Arc responses are disrupted in a mouse model of Alzheimer's disease. *Nat Neurosci* **15**, 1422-1429

68. Rudinskiy, N., Hawkes, J. M., Wegmann, S., Kuchibhotla, K. V., Muzikansky, A., Betensky, R. A., Spires-Jones, T. L., and Hyman, B. T. (2014) Tau pathology does not affect experience-driven single-neuron and network-wide Arc/Arg3.1 responses. *Acta Neuropathol Commun* **2**, 63

69. Schulz, L., Ramirez, P., Lemieux, A., Gonzalez, E., Thomson, T., and Frost, B. (2022) Tau-Induced Elevation of the Activity-Regulated Cytoskeleton Associated Protein Arc1 Causally Mediates Neurodegeneration in the Adult Drosophila Brain. *Neuroscience*

70. Steward, O., Wallace, C. S., Lyford, G. L., and Worley, P. F. (1998) Synaptic activation causes the mRNA for the IEG Arc to localize selectively near activated postsynaptic sites on dendrites. *Neuron* **21**, 741-751
71. Moga, D. E., Calhoun, M. E., Chowdhury, A., Worley, P., Morrison, J. H., and Shapiro, M. L. (2004) Activity-regulated cytoskeletal-associated protein is localized to recently activated excitatory synapses. *Neuroscience* **125**, 7-11
72. Ramirez-Amaya, V., Vazdarjanova, A., Mikhael, D., Rosi, S., Worley, P. F., and Barnes, C. A. (2005) Spatial exploration-induced Arc mRNA and protein expression: evidence for selective, network-specific reactivation. *J Neurosci* **25**, 1761-1768
73. Petrucelli, L., Dickson, D., Kehoe, K., Taylor, J., Snyder, H., Grover, A., De Lucia, M., McGowan, E., Lewis, J., Prihar, G., Kim, J., Dillmann, W. H., Browne, S. E., Hall, A., Voellmy, R., Tsuboi, Y., Dawson, T. M., Wolozin, B., Hardy, J., and Hutton, M. (2004) CHIP and Hsp70 regulate tau ubiquitination, degradation and aggregation. *Hum Mol Genet* **13**, 703-714
74. Eriksen, M. S., Nikolaienko, O., Hallin, E. I., Grodem, S., Bustad, H. J., Flydal, M. I., Merski, I., Hosokawa, T., Lascu, D., Akerkar, S., Cuellar, J., Chambers, J. J., O'Connell, R., Muruganandam, G., Loris, R., Touma, C., Kanhema, T., Hayashi, Y., Stratton, M. M., Valpuesta, J. M., Kursula, P., Martinez, A., and Bramham, C. R. (2021) Arc self-association and formation of virus-like capsids are mediated by an N-terminal helical coil motif. *FEBS J* **288**, 2930-2955
75. Ashley, J., Cordy, B., Lucia, D., Fradkin, L. G., Budnik, V., and Thomson, T. (2018) Retrovirus-like Gag Protein Arc1 Binds RNA and Traffics across Synaptic Boutons. *Cell* **172**, 262-274 e211
76. Pastuzyn, E. D., Day, C. E., Kearns, R. B., Kyrke-Smith, M., Taibi, A. V., McCormick, J., Yoder, N., Belnap, D. M., Erlendsson, S., Morado, D. R., Briggs, J. A. G., Feschotte, C., and Shepherd, J. D. (2018) The Neuronal Gene Arc Encodes a Repurposed Retrotransposon Gag Protein that Mediates Intercellular RNA Transfer. *Cell* **173**, 275

77. Boratyn, G. M., Schaffer, A. A., Agarwala, R., Altschul, S. F., Lipman, D. J., and Madden, T. L. (2012) Domain enhanced lookup time accelerated BLAST. *Biol Direct* **7**, 12
78. Hallin, E. I., Eriksen, M. S., Baryshnikov, S., Nikolaienko, O., Grodem, S., Hosokawa, T., Hayashi, Y., Bramham, C. R., and Kursula, P. (2018) Structure of monomeric full-length ARC sheds light on molecular flexibility, protein interactions, and functional modalities. *J Neurochem* **147**, 323-343
79. Liu, C., Song, X., Nisbet, R., and Gotz, J. (2016) Co-immunoprecipitation with Tau Isoform-specific Antibodies Reveals Distinct Protein Interactions and Highlights a Putative Role for 2N Tau in Disease. *J Biol Chem* **291**, 8173-8188
80. Hori, T., Eguchi, K., Wang, H. Y., Miyasaka, T., Guillaud, L., Taoufiq, Z., Mahapatra, S., Yamada, H., Takei, K., and Takahashi, T. (2022) Microtubule assembly by tau impairs endocytosis and neurotransmission via dynamin sequestration in Alzheimer's disease synapse model. *Elife* **11**
81. Ittner, A., and Ittner, L. M. (2018) Dendritic Tau in Alzheimer's Disease. *Neuron* **99**, 13-27
82. Regan, P., Piers, T., Yi, J. H., Kim, D. H., Huh, S., Park, S. J., Ryu, J. H., Whitcomb, D. J., and Cho, K. (2015) Tau phosphorylation at serine 396 residue is required for hippocampal LTD. *J Neurosci* **35**, 4804-4812
83. Kimura, T., Whitcomb, D. J., Jo, J., Regan, P., Piers, T., Heo, S., Brown, C., Hashikawa, T., Murayama, M., Seok, H., Sotiropoulos, I., Kim, E., Collingridge, G. L., Takashima, A., and Cho, K. (2014) Microtubule-associated protein tau is essential for long-term depression in the hippocampus. *Philos Trans R Soc Lond B Biol Sci* **369**, 20130144
84. Suzuki, M., and Kimura, T. (2017) Microtubule-associated tau contributes to intra-dendritic trafficking of AMPA receptors in multiple ways. *Neurosci Lett* **653**, 276-282
85. Franchini, L., Stanic, J., Ponzoni, L., Mellone, M., Carrano, N., Musardo, S., Zianni, E., Olivero, G., Marcello, E., Pittaluga, A., Sala, M., Bellone, C., Racca, C., Di Luca, M., and Gardoni, F. (2019) Linking NMDA Receptor Synaptic Retention to Synaptic Plasticity and Cognition. *iScience* **19**, 927-939

86. Hoover, B. R., Reed, M. N., Su, J., Penrod, R. D., Kotilinek, L. A., Grant, M. K., Pitstick, R., Carlson, G. A., Lanier, L. M., Yuan, L. L., Ashe, K. H., and Liao, D. (2010) Tau mislocalization to dendritic spines mediates synaptic dysfunction independently of neurodegeneration. *Neuron* **68**, 1067-1081
87. Gamache, J., Benzow, K., Forster, C., Kemper, L., Hlynialuk, C., Furrow, E., Ashe, K. H., and Koob, M. D. (2019) Factors other than hTau overexpression that contribute to tauopathy-like phenotype in rTg4510 mice. *Nat Commun* **10**, 2479
88. Goodwin, L. O., Splinter, E., Davis, T. L., Urban, R., He, H., Braun, R. E., Chesler, E. J., Kumar, V., van Min, M., Ndukum, J., Philip, V. M., Reinholdt, L. G., Svenson, K., White, J. K., Sasner, M., Lutz, C., and Murray, S. A. (2019) Large-scale discovery of mouse transgenic integration sites reveals frequent structural variation and insertional mutagenesis. *Genome Res* **29**, 494-505
89. Bachmann, S., Bell, M., Klimek, J., and Zempel, H. (2021) Differential Effects of the Six Human TAU Isoforms: Somatic Retention of 2N-TAU and Increased Microtubule Number Induced by 4R-TAU. *Front Neurosci* **15**, 643115
90. Liu, C., and Gotz, J. (2013) Profiling murine tau with 0N, 1N and 2N isoform-specific antibodies in brain and peripheral organs reveals distinct subcellular localization, with the 1N isoform being enriched in the nucleus. *PLoS One* **8**, e84849
91. Cherry, J. D., Esnault, C. D., Baucom, Z. H., Tripodis, Y., Huber, B. R., Alvarez, V. E., Stein, T. D., Dickson, D. W., and McKee, A. C. (2021) Tau isoforms are differentially expressed across the hippocampus in chronic traumatic encephalopathy and Alzheimer's disease. *Acta Neuropathol Commun* **9**, 86
92. Alonso, A. D., Zaidi, T., Novak, M., Barra, H. S., Grundke-Iqbal, I., and Iqbal, K. (2001) Interaction of tau isoforms with Alzheimer's disease abnormally hyperphosphorylated tau and in vitro phosphorylation into the disease-like protein. *J Biol Chem* **276**, 37967-37973
93. Goedert, M., and Jakes, R. (1990) Expression of separate isoforms of human tau protein: correlation with the tau pattern in brain and effects on tubulin polymerization. *EMBO J* **9**, 4225-4230

94. Lee, V. M., Goedert, M., and Trojanowski, J. Q. (2001) Neurodegenerative tauopathies. *Annu Rev Neurosci* **24**, 1121-1159

95. Hall, A. M., and Roberson, E. D. (2012) Mouse models of Alzheimer's disease. *Brain Res Bull* **88**, 3-12

96. Gamache, J. E., Kemper, L., Steuer, E., Leinonen-Wright, K., Choquette, J. M., Hlynialuk, C., Benzow, K., Vossel, K. A., Xia, W., Koob, M. D., and Ashe, K. H. (2020) Developmental Pathogenicity of 4-Repeat Human Tau Is Lost with the P301L Mutation in Genetically Matched Tau-Transgenic Mice. *J Neurosci* **40**, 220-236

97. Cohen, T. J., Constance, B. H., Hwang, A. W., James, M., and Yuan, C. X. (2016) Intrinsic Tau Acetylation Is Coupled to Auto-Proteolytic Tau Fragmentation. *PLoS One* **11**, e0158470

98. Ho, S. N., Hunt, H. D., Horton, R. M., Pullen, J. K., and Pease, L. R. (1989) Site-directed mutagenesis by overlap extension using the polymerase chain reaction. *Gene* **77**, 51-59

Figure Legends:

Figure 1: WT-tau but not P301L-tau decreases Arc in HEK 293 cells.

A, Schematic showing the structure of human tau. The longest isoform 2N4R, has 2 N-terminal repeats and 4 Microtubule-binding Domain (MTBD) repeats. The 0N4R isoform has no N-terminal repeats and 4 MTBD repeats, while the 0N3R isoform has no N-terminal repeats and 3 MTBD repeats. The P301L and P301S mutations are located in the R2 MTBD.

B, *Top,* Representative western blots showing the levels of myc-Arc with increasing concentrations of GFP-tau (0N4R) in HEK293 cells (0, 0.25, 0.5, 0.75, 1 and 1.5 µg). Actin was used as a loading control. *Bottom,* Quantification of myc-Arc levels normalized to actin showing a significant decrease in Arc with increasing Tau. Kruskal-Wallis, $p = 0.0009$.

C, *Top,* Representative western blots showing the levels of myc-Arc with increasing concentrations of GFP-P301L tau in HEK293 cells (0, 0.25, 0.5, 0.75, 1 and 1.5 µg). Actin was used as a loading control. *Bottom,* Quantification of myc-Arc levels normalized to actin showing no significant differences in Arc with increasing P301L Tau. One-way ANOVA, $F(5,18) = 0.3018$, $p = 0.3$.

D, *Top,* Representative western blots showing the levels of myc-Arc with increasing concentrations of GFP-P301S tau in HEK293 cells (0, 0.25, 0.5, 0.75, 1 and 1.5 µg). Actin was used as a loading control. *Bottom,* Quantification of myc-Arc levels normalized to actin showing a significant decrease in Arc with increasing P301S tau. One-way ANOVA, $F(5,18) = 10.96$, $p < 0.0001$.

E, *Top,* Representative western blots showing the levels of myc-Arc with increasing concentrations of 0N3R tau transfected in HEK293 cells (0, 0.25, 0.5, 0.75, 1 and 1.5 µg). Actin was used as a loading control. *Bottom,* Quantification of myc-Arc levels normalized to actin. One-way ANOVA $F(5,18) = 0.034$, $p = 0.999$.

Figure 2: Tau modulation of Arc requires proteasome activity but does not increase Arc ubiquitination.

A, Following transfection, cells were treated with either Vehicle (DMSO) or MG-132 (10 mM) for 4 hours. *Left, r*epresentative western blots showing myc-Arc with increasing concentrations of GFP-tau in DMSO treated HEK293 cells (0, 0.25, 0.5, 0.75, 1 and 1.5 µg). Actin was used as a loading control. *Right*, *r*epresentative western blots showing myc-Arc with increasing concentrations of GFP-tau in DMSO treated HEK293 cells (0, 0.25, 0.5, 0.75, 1 and 1.5 µg). Actin was used as a loading control.

B, Quantification of myc-Arc levels normalized to actin showing a significant decrease in Arc with increasing Tau in vehicle-treated cells (left), but not in the MG-132-treated cells (right). One-way ANOVA for DMSO control, $F(5,12) = 4.03$, $p = 0.022$; one-way ANOVA for MG-132, $F(5,12) = 1.9$, $p = 0.15$.

C, Schematic showing the structure of Arc, highlighting the coiled-coil (CC) domain and the endophilin-binding (EB) domain on the N-terminus, and the N- and C-lobe on the C-terminus. The locations of the lysines (K55,136, 268, 269 and 293) targeted for ubiquitination by RNF216 and UBE3A are shown.

D, *Left,* Representative western blots showing myc-Arc5KR (K55,136, 268, 269 and 293 mutated to Arginine) with increasing concentrations of GFP-tau in HEK293 cells (0, 0.25, 0.5, 0.75, 1 and 1.5 µg). Actin was used as a loading control. *Right*, Quantification of myc-Arc5KR levels normalized to actin showing a significant decrease in Arc with increasing tau. One-way ANOVA $F = (5,18) = 6.4$, $p = 0.0014$.

E, *Top,* Ubiquitin assay showing no enhancement in Arc ubiquitination when co-expressed with Tau or P301L tau. RNF216 was used as a positive control. *Bottom*, Input showing expression of myc-Arc, GFP-RNF216, GFP-tau and GFP-P301L tau.

F, Coimmunoprecipitation assay showing pulldown of myc-Arc with anti-myc antibody and immunoblotting with an anti-GFP antibody. GFP-RNF216 was used as a positive control.

Figure 3: Tau does not enhance lysosomal degradation of Arc

A, Representative western blots showing myc-Arc expressed alone or with GFP-tau. Cells were treated with Vehicle (water) or a combination of leupeptin (50 µM) and ammonium (10 mM) chloride for 6 hr to block lysosome degradation. Actin was used as

a loading control. Blots showing markers for lysosome inhibition, LC3 and p62/SQSTM1 with total protein stain used as a loading control.

B, Quantification of myc-Arc showing a significant decrease with co-expression of GFP-tau in Vehicle and following lysosome inhibition. t-test for vehicle control, $t = 10.6$, $df = 10$, ****$p < 0.0001$; unpaired t-test for inhibitors, $t = 5.585$, $df = 10$, $p = 0.0002$.

C, Quantification of LC3 and p62/SQSTM1 showing a significant increase of LC3 (unpaired t-test, $t = 12.52$, $df = 22$, ****$p < 0.0001$) and p62/SQSTM1 (unpaired t-test, $t = 10.54$, $df = 22$, ****$p < 0.0001$) in cells treated with inhibitors.

D, Representative western blots showing RIPA-soluble and insoluble fractions of myc-Arc expressed alone or with GFP-tau.

Figure 4: Tau-induced Arc removal does not depend on GSK3α/β Arc phosphorylation

A, *Left,* Representative western blots showing myc-Arc expressed alone or with GFP-tau. Cells were treated with Vehicle (Water) or CH98 (1-2 μM) for 4 h. Actin was used as a loading control. Right, Quantification of myc-Arc showing a significant decrease with co-expression of GFP-tau after treatment with Vehicle (unpaired t-test, $t = 3.450$, $df = 18$, $p = 0.0029$) or CH98 (unpaired t-test, $t = 3.417$, $df = 18$, $p = 0.0031$).

B, Schematic showing the structure of Arc with the location of mapped GSK3α/β phosphorylation sites S170, T175, T368 and T380.

C-E, *Left,* Representative western blots showing myc-Arc S170A/T175A, myc-Arc T368A, or myc-Arc T380A with Arc phosphorylation sites mutated to Alanine expressed alone or with GFP-tau. Actin was used as a loading control. *Right,* Quantification of myc-Arc S170A/T175A, myc-Arc T368A, or myc-Arc T380A showing a significant decrease when co-expressed with Tau. Unpaired t-test for Arc S170A/T175A, $t = 4.913$, $df = 16$, $p = 0.0002$; Unpaired t-test for Arc T368A, $t = 8.714$, $df = 4$, $p = 0.001$; Unpaired t-test for Arc T380A, $t = 11.59$, $df = 4$, $p = 0.0003$.

Figure 5: The Endophilin-binding domain of Arc is essential for tau-induced degradation

A, Schematic showing the structure of Arc, highlighting the coiled-coil (CC) domain and the endophilin-binding (EB) domain on the N-terminus, and the N- and C-lobe on the C-terminus. The location of the K92 acetylation site is shown.

B-E, *Left,* Representative western blots showing WT myc-Arc, myc-Arc ∆C-terminal (lacking the C-terminal domain), myc-Arc ∆CC (lacking the coiled-coil motif on the N-terminal domain), and myc-Arc ∆EB (lacking the endophilin-binding domain on the N-terminus). expressed alone or with GFP-tau. Actin and tubulin were used as loading controls. *Right,* Quantification of WT myc-Arc, myc-Arc ∆C-terminal, myc-Arc ∆CC, and myc-Arc ∆EB. Only Arc ∆EB does not show a decrease with Tau overexpression (Unpaired t-test for WT Arc $t = 8.857$, $df = 10$, ****$p < 0.0001$; Unpaired t-test for Arc ∆C-terminal $t = 6.471$, df =1 0, ****$p < 0.0001$; Unpaired t-test for Arc ∆CC $t = 7.076$, $df = 10$, ****$p < 0.0001$; Unpaired t-test Arc ∆EB $t = 0.2956$, $df = 10$, $p = 0.774$).

F, *Left,* Representative western blots showing myc-Arc K92Q with the acetylation site K92 mutated to glutamine expressed alone or with GFP-tau. Actin was used as a loading control. *Right,* Quantification of myc- Arc K92Q showing a significant decrease when co-expressed with Tau. Unpaired t-test $t = 5.54$, $df = 10$, $p = 0.0002$

Figure 6: GFP-tau but not GFP-P301L tau degrades endogenous Arc in primary hippocampal neurons

A, Primary hippocampal neurons transfected with GFP or increasing concentrations of GFP-tau (X= 0.25 µg, 2X = 0.5 µg, 4X = 1.0 µg), and GFP-P301L tau (2X = 0.5 µg). Td-tomato was used to outline neuron morphology. Scale bar represents 20 µm.

B, Quantification of Arc protein (magenta) in soma and dendrites showing a decrease in Arc selectively in dendrites with increasing tau concentrations but not with GFP-P301L. One-way ANOVA in dendrites $F(4,88) = 4.4$, $p = 0.0027$, Tukey's post-hoc GFP vs. 2X Tau $p = 0.0042$, GFP vs. 4X Tau $p = 0.013$; one-way ANOVA in soma $F(4,99) = 1.342$, $p = 0.259$.

Figure 7: Tau degradation of dendritic Arc in primary hippocampal neurons is proteasome dependent

A, Primary hippocampal neurons overexpressing GFP or GFP-tau. Td-tomato was used to outline neuron morphology. Cells treated with either Vehicle (DMSO) or MG-132 (10 μM) for 4 h. Scale bar represents 20 μm.

B, Quantification of Arc protein (magenta) in soma and apical dendrites showing a decrease in Arc selectively in dendrites with increasing tau concentrations in cultures treated with Vehicle but not in cultures treated with MG-132. Unpaired t-test DMSO Control in dendrites $t=2.72$, $df = 27$, $p = 0.011$; Unpaired t-test MG-132 in dendrites $t = 0.3814$, $df = 27$ $p = 0.706$; Unpaired t-test DMSO in soma $t = 1.044$, $df = 27$, $p = 0.306$; Unpaired t-test MG-132 in soma $t = 0.16$, $df = 27$, $p = 0.874$.

Figure 8: GFP-tau but not GFP-P301L tau overexpression increases surface GluA1 in dendrites and in the soma.

A, Primary hippocampal neurons overexpressing GFP, GFP-tau and GFP-P301L tau. Td-tomato was used to outline neuron morphology. Scale bar represents 20 μm. Scale bar for selected dendrites represents 10 μm.

B, Quantification of surface GluA1 (magenta) in soma and apical dendrites. Kruskal-Wallis test for dendrites, $p = 0.0458$; Kruskal-Wallis test for soma, $p = 0.0034$.

Figure 1

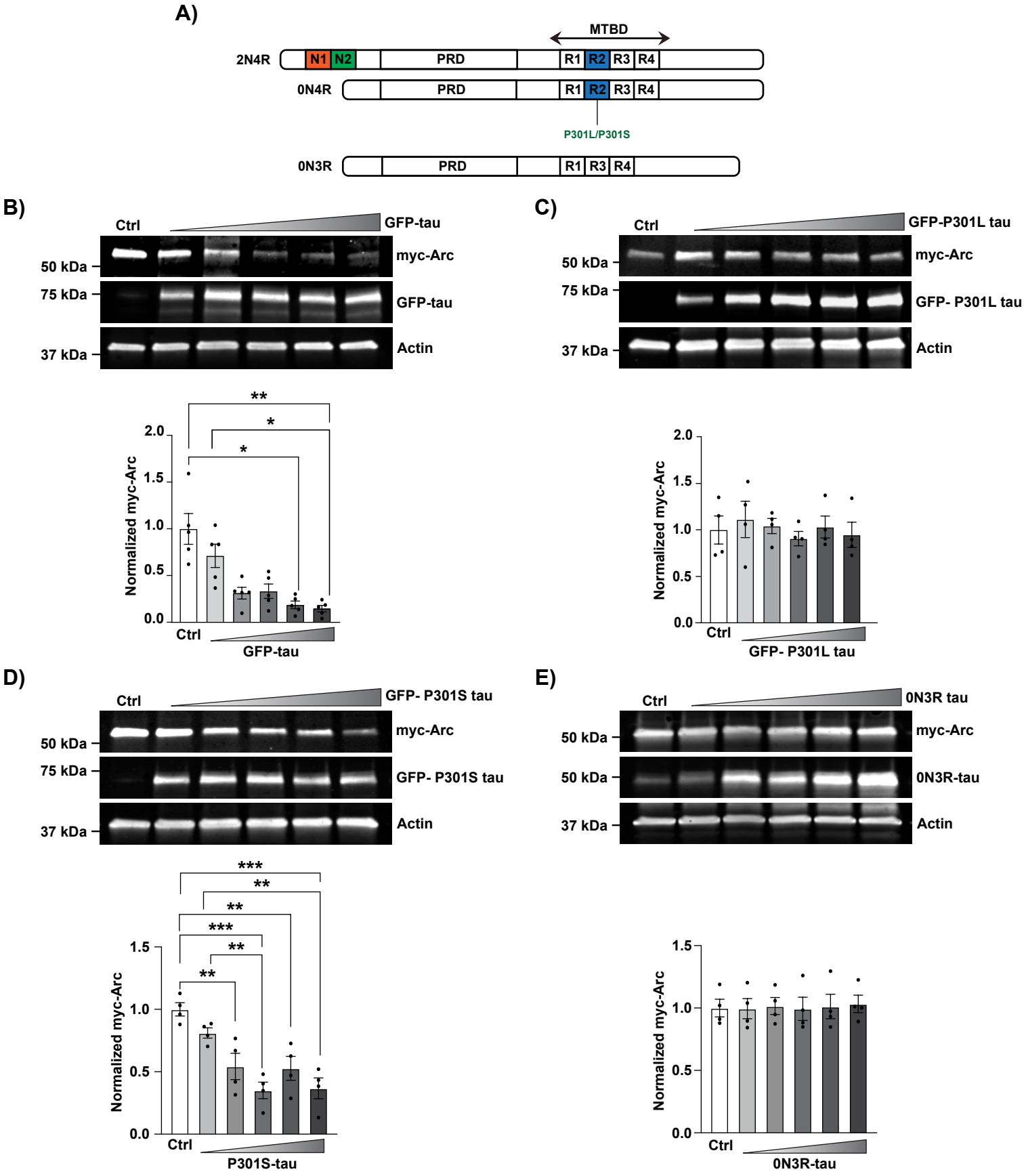
A)
MTBD
2N4R
N1
N2
PRD
R1
R2
R3
R4
0N4R
P301L/P301S
0N3R
B)
Ctrl
GFP-tau
50 kDa
75 kDa
37 kDa
myc-Arc
GFP-tau
Actin
Normalized myc-Arc
C)
GFP-P301L tau
GFP- P301L tau
D)
GFP- P301S tau
P301S-tau
E)
0N3R tau
0N3R-tau

Figure 2

A)

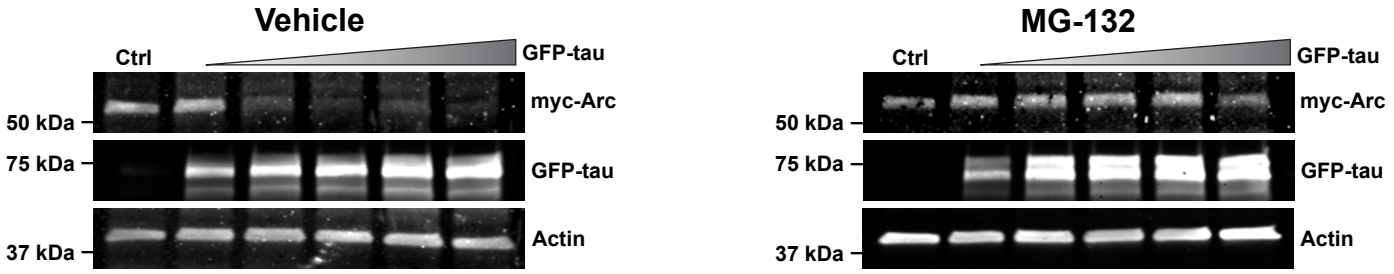

B)

C)

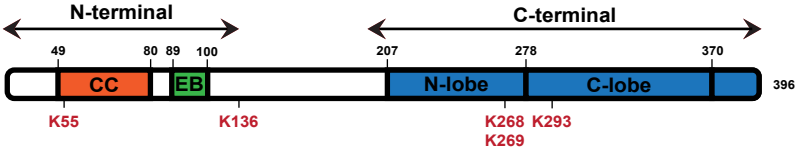

D)

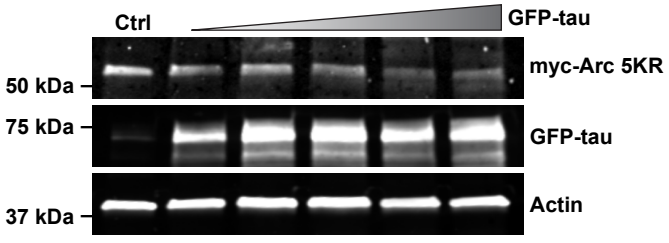

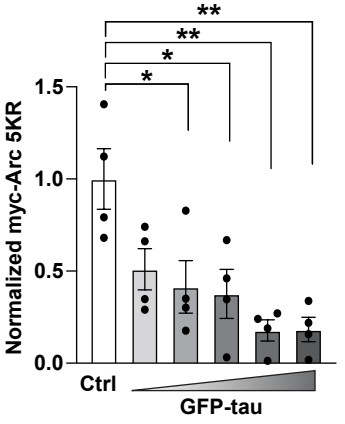

E)

pcDNA3.1	+	+	-	-	-
myc-Arc	-	+	+	+	+
GFP-RNF216	-	-	+	-	-
GFP-tau	-	-	-	+	-
GFP-P301L tau	-	-	-	-	+

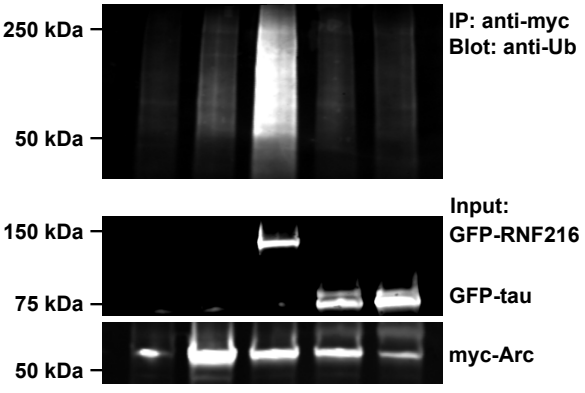

F)

pcDNA3.1	+	+	-	-	-
myc-Arc	-	-	+	+	+
GFP-RNF216	-	-	+	-	-
GFP-tau	-	+	-	+	-
GFP-P301L tau	-	-	-	-	+

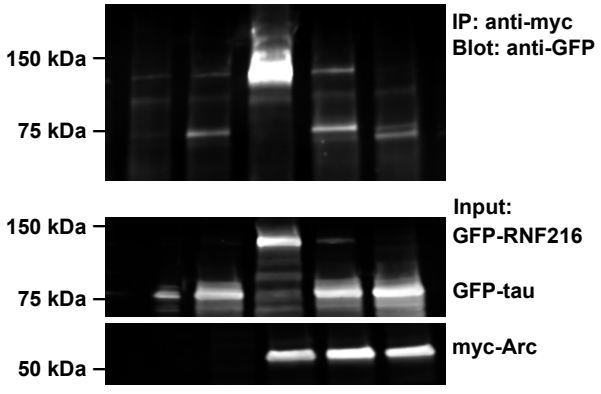

Figure 3

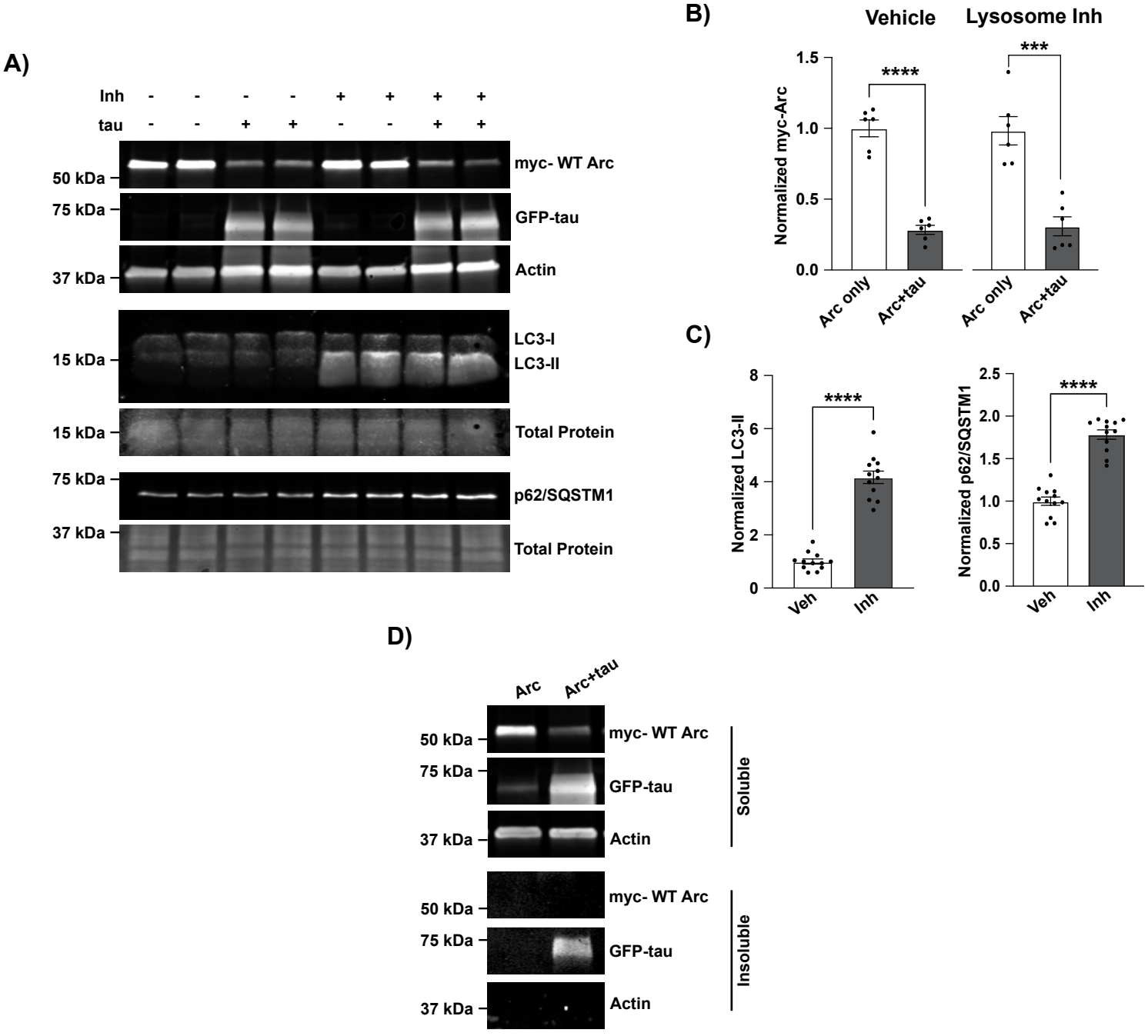
A)
Inh - - - - + + + +
tau - - + + - - + +
50 kDa
75 kDa
37 kDa
myc- WT Arc
GFP-tau
Actin
15 kDa
LC3-I
LC3-II
15 kDa
Total Protein
75 kDa
p62/SQSTM1
37 kDa
Total Protein
B)
Vehicle
Lysosome Inh
Normalized myc-Arc
1.5
1.0
0.5
0.0
****
***
Arc only
Arc+tau
Arc only
Arc+tau
C)
Normalized LC3-II
8
6
4
2
0
****
Veh
Inh
Normalized p62/SQSTM1
2.5
2.0
1.5
1.0
0.5
0.0
****
Veh
Inh
D)
Arc
Arc+tau
50 kDa
75 kDa
37 kDa
myc- WT Arc
GFP-tau
Actin
Soluble
50 kDa
75 kDa
37 kDa
myc- WT Arc
GFP-tau
Actin
Insoluble

Figure 4

A)

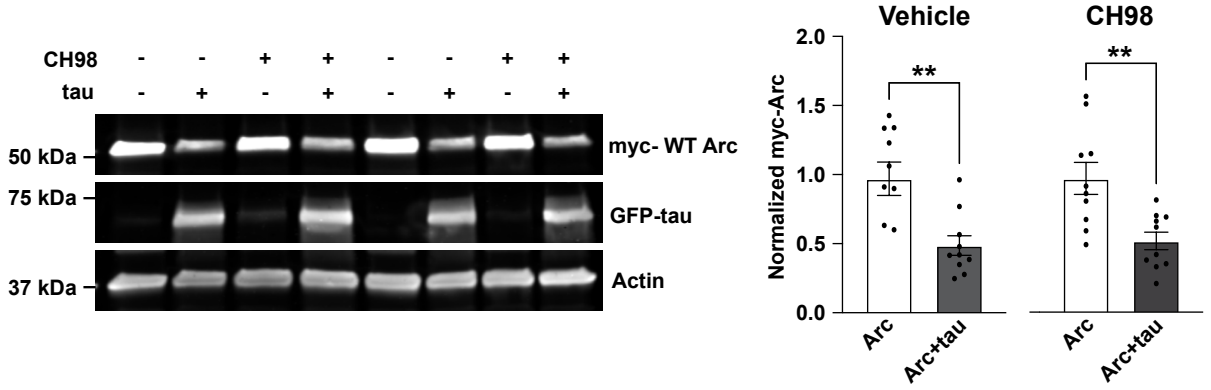

B)

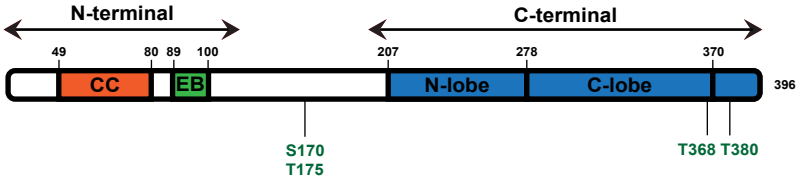

C)

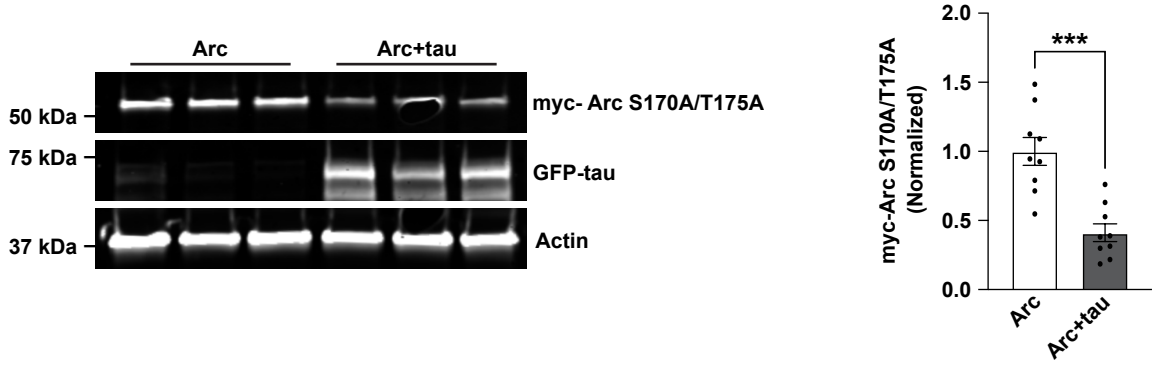

D)

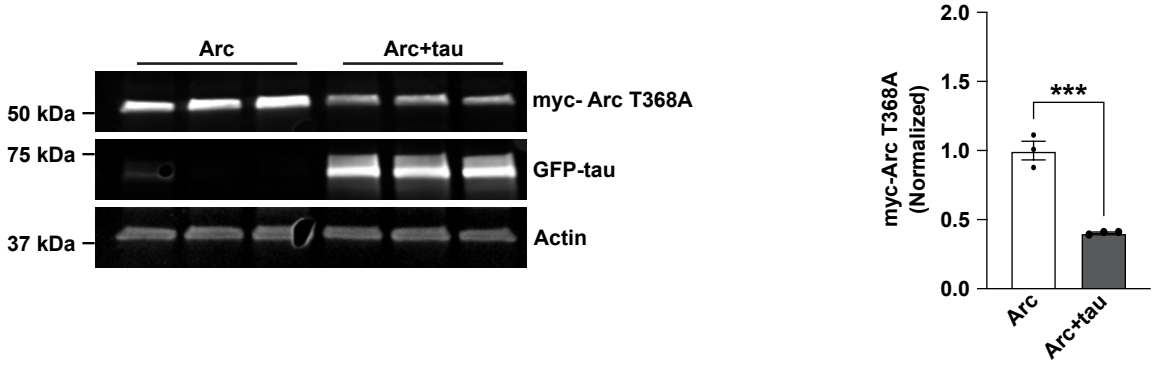

E)

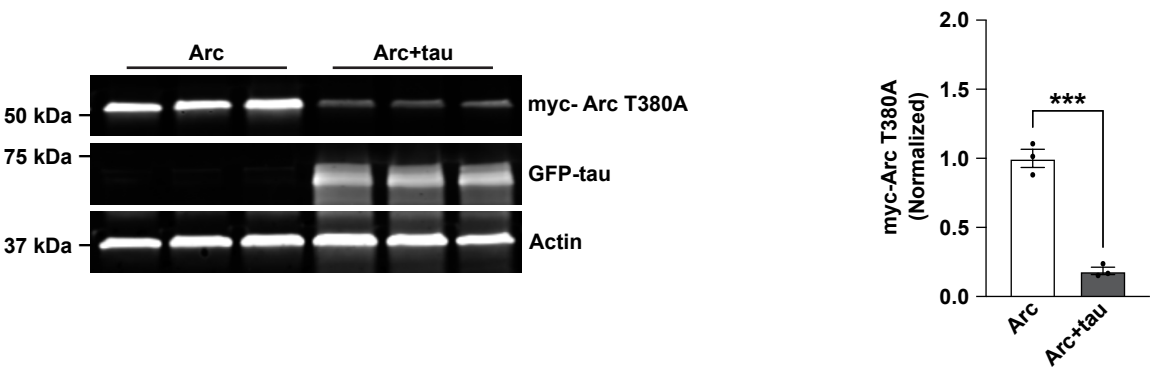

Figure 5

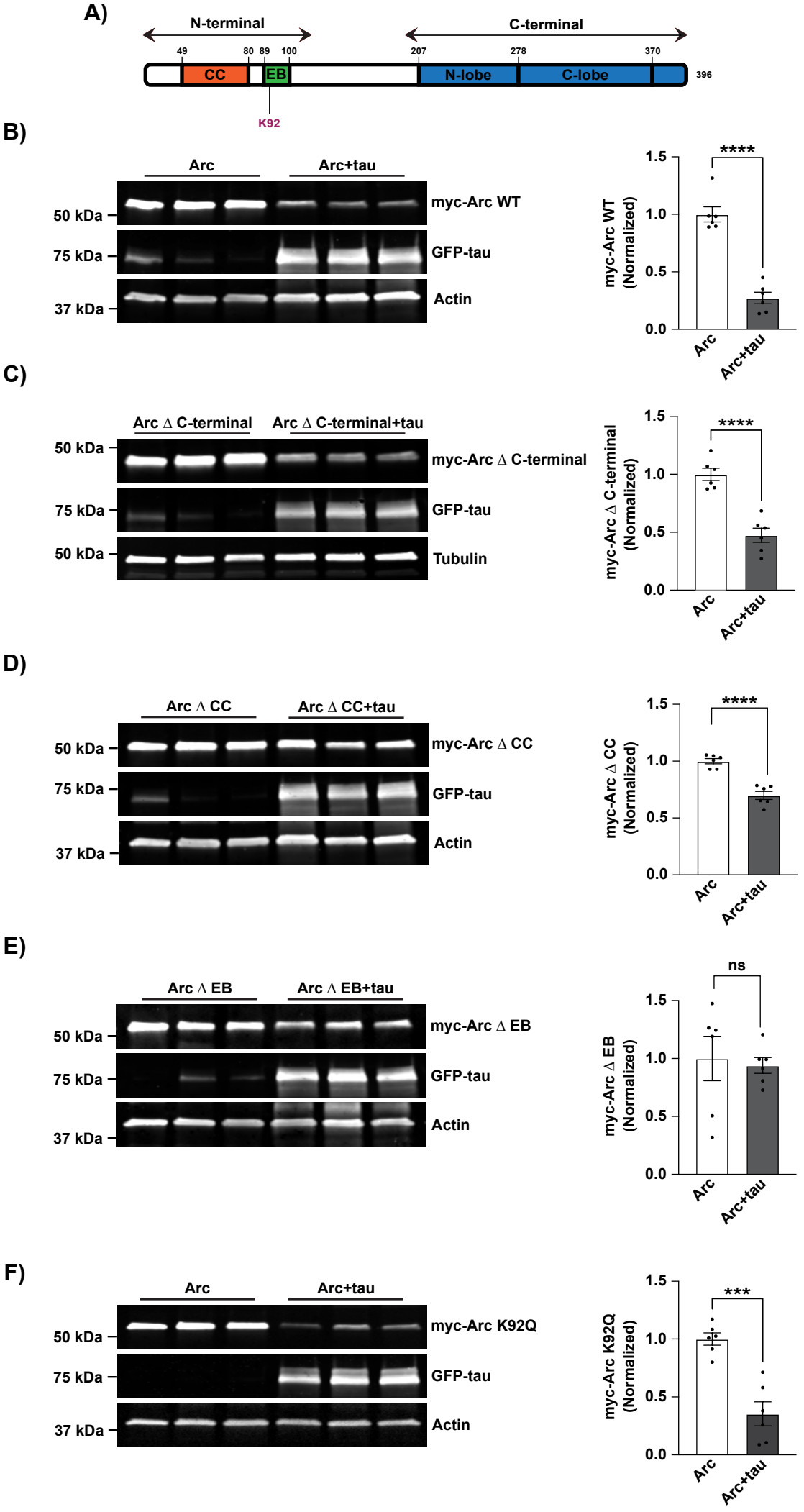
A)
N-terminal
C-terminal
49
80
89
100
207
278
370
396
CC
EB
N-lobe
C-lobe
K92
B)
Arc
Arc+tau
50 kDa
75 kDa
37 kDa
myc-Arc WT
GFP-tau
Actin
myc-Arc WT (Normalized)
****
C)
Arc Δ C-terminal
Arc Δ C-terminal+tau
50 kDa
75 kDa
50 kDa
myc-Arc Δ C-terminal
GFP-tau
Tubulin
myc-Arc Δ C-terminal (Normalized)
****
D)
Arc Δ CC
Arc Δ CC+tau
50 kDa
75 kDa
37 kDa
myc-Arc Δ CC
GFP-tau
Actin
myc-Arc Δ CC (Normalized)
****
E)
Arc Δ EB
Arc Δ EB+tau
50 kDa
75 kDa
37 kDa
myc-Arc Δ EB
GFP-tau
Actin
myc-Arc Δ EB (Normalized)
ns
F)
Arc
Arc+tau
50 kDa
75 kDa
37 kDa
myc-Arc K92Q
GFP-tau
Actin
myc-Arc K92Q (Normalized)
***
1.5
1.0
0.5
0.0
Arc
Arc+tau

Figure 6

A)

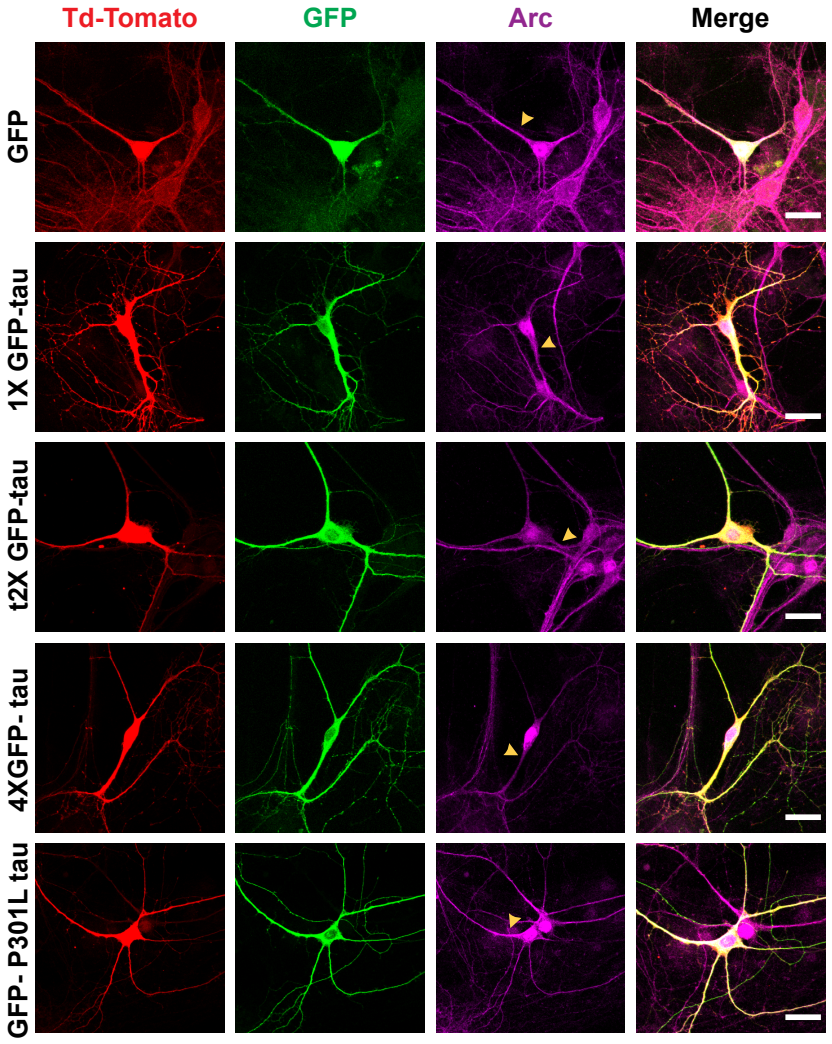
Td-Tomato
GFP
Arc
Merge
GFP
1X GFP-tau
t2X GFP-tau
4XGFP- tau
GFP- P301L tau

B)

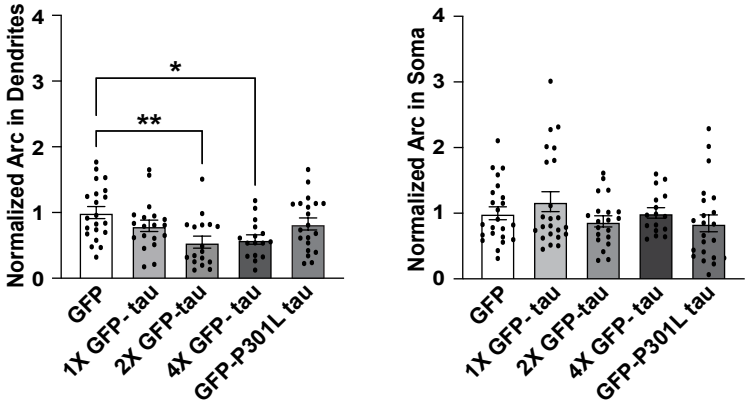
Normalized Arc in Dendrites
0
1
2
3
4
*
**
GFP
1X GFP- tau
2X GFP-tau
4X GFP- tau
GFP-P301L tau
Normalized Arc in Soma
0
1
2
3
4
GFP
1X GFP- tau
2X GFP-tau
4X GFP- tau
GFP-P301L tau

Figure 7

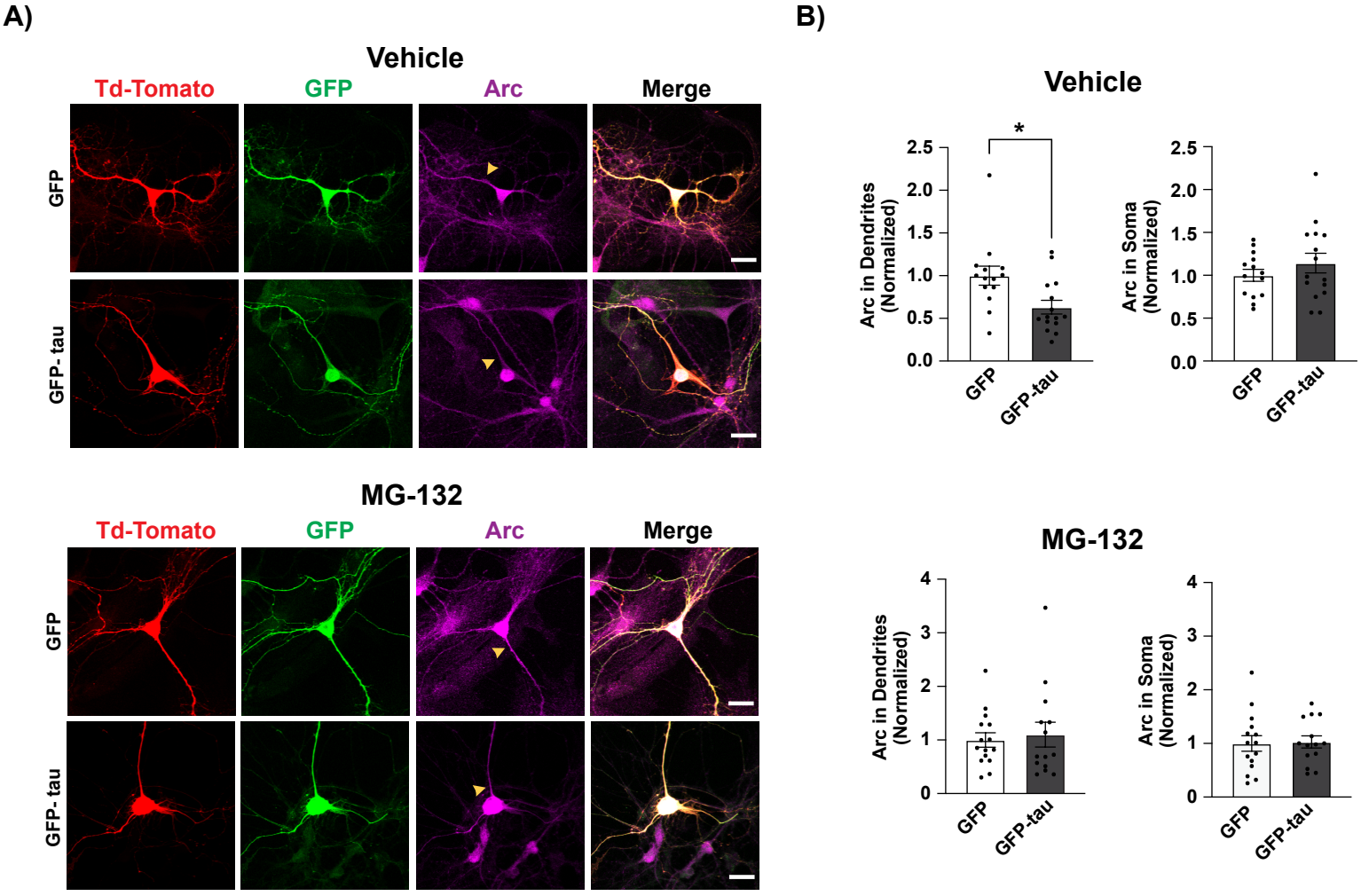
A)
Vehicle
Td-Tomato
GFP
Arc
Merge
GFP
GFP- tau
MG-132
Td-Tomato
GFP
Arc
Merge
GFP
GFP- tau
B)
Vehicle
*
Arc in Dendrites (Normalized)
2.5
2.0
1.5
1.0
0.5
0.0
GFP
GFP-tau
Arc in Soma (Normalized)
2.5
2.0
1.5
1.0
0.5
0.0
GFP
GFP-tau
MG-132
Arc in Dendrites (Normalized)
4
3
2
1
0
GFP
GFP-tau
Arc in Soma (Normalized)
4
3
2
1
0
GFP
GFP-tau

Figure 8

A)

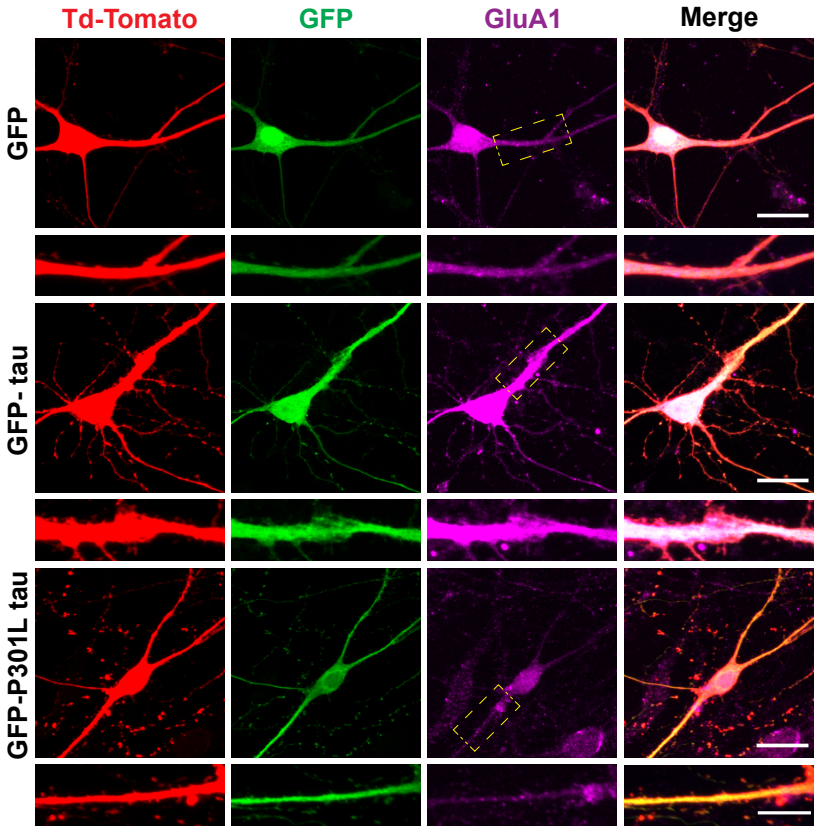
Td-Tomato
GFP
GluA1
Merge
GFP
GFP- tau
GFP-P301L tau

B)

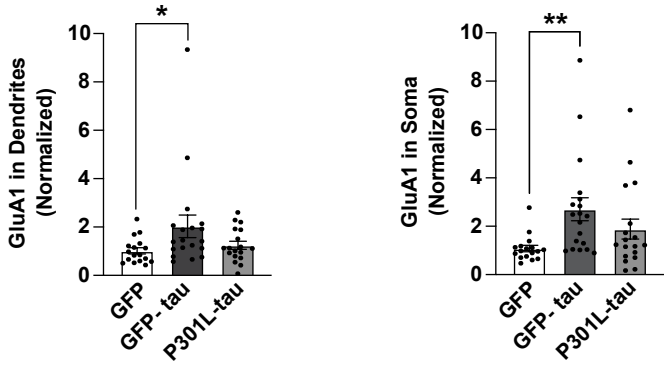
GluA1 in Dendrites (Normalized)
*
10
8
6
4
2
0
GFP
GFP- tau
P301L-tau
GluA1 in Soma (Normalized)
**
10
8
6
4
2
0
GFP
GFP- tau
P301L-tau